CELLULAR INACTIVATION USING NANOSECOND PULSED ELECTRIC FIELDS

by

Aginiprakash Dhanabal

A Thesis

Submitted to the Faculty of Purdue University

In Partial Fulfillment of the Requirements for the degree of

Master of Science in Agricultural and Biological Engineering

School of Agricultural & Biological Engineering

West Lafayette, Indiana

May 2020

THE PURDUE UNIVERSITY GRADUATE SCHOOL
STATEMENT OF COMMITTEE APPROVAL

Dr. Allen L. Garner, Chair

School of Nuclear Engineering

Dr. David A. Detwiler

Nanovis, LLC

Dr. Kevin V. Solomon

Department of Agricultural and Biological Engineering

Approved by:

Dr. Nathan Mosier

Head of the Graduate Program

To my parents, friends and advisors that inspired me to pursue novel scientific exploration.

ACKNOWLEDGMENTS

I would like to express my very great appreciation to Dr. Allen Garner for his valuable and constructive suggestions during the planning and development of this research work. His willingness to give his time so generously has been very much appreciated. This work could not have happened without the constant support and encouragement of Dr. David Detwiler. I would also like to thank Dr. Kevin Solomon for the thought-provoking questions and reviewing efforts.

I would also like add a special thanks to Dr. Anand Vadlamani for guiding me and supporting me both in and out of lab over the past few years.

TABLE OF CONTENTS

LIST OF TABLES

LIST OF FIGURES

ABSTRACT

Author: Dhanabal, Aginiprakash. MS
Institution: Purdue University
Degree Received: May 2020
Title: Cellular Inactivation using Nanosecond Pulsed Electric Fields
Committee Chair: Allen Garner

Pulsed electric fields (PEFs) can induce numerous biophysical phenomena, especially perturbation of the outer and inner membranes, that may be used for applications that include nonthermal pasteurization, enhanced permeabilization of tumors to improve the transport of chemotherapeutics for cancer therapy, and enhanced membrane permeabilization of individual cells to enhance RNA and DNA delivery for gene therapy. The applied electric field and pulse duration determine the density, size, and reversibility of the created membrane pores. PEFs with durations longer than the outer membrane's charging time will induce pore formation with the potential for application in irreversible electroporation for cancer therapy and microorganism inactivation. Shorter duration PEFs, particularly on the nanosecond timescale (nsPEFs), induce a larger density of smaller membrane pores with the potential to permeabilize intracellular membranes, such as the mitochondria, to induce programmed cell death. Thus, the PEFs can effectively kill multiple types of cells, dependent upon the cells. This thesis assesses the ability of nsPEFs to kill different cell types, specifically microorganisms with and without antibiotics as well as varying the parameters to affect populations of immortalized leukemia cells (Jurkats).

Antibiotic resistance has been an acknowledged challenge since the initial development of penicillin; however, recent discoveries by the CDC and the WHO of microorganisms resistant to last line of defense drugs combined with predictions of potential infection cases reaching 50 million a year globally and the absence new drugs in the discovery pipeline highlight the need to develop novel ways to combat and overcome these resistance mechanisms. Repurposing drugs, exploring nature for new drugs, and developing enzymes to counter the resistance mechanisms may provide potential alternatives for addressing the scarcity of antibiotics effective against gram-negative infections. One may also leverage the abundance of drugs effective against gram-positive infections by using nsPEFs to make them effective against gram-negative infections, including

bacterial species with multiple natural and acquired resistance mechanisms. Numerous drug and microbial combinations for different doses and pulse treatments were tested and presented here.

Low intensity PEFs may selectively target cell populations at different stages of the cell cycle (quiescence and mitosis) to modify cancer cell population dynamics. Experimental studies of cancer cell growth when exposed to a low number of nsPEFs, while varying pulse duration, field intensity and number of pulses reveals a threshold beyond which cell recovery is not possible, but also a point of diminishing returns if cell death is the intention. A theory comprised of coupled differential equations representing the proliferating and quiescent cells showed how changing PEF parameters altered the behavior of these cell populations after treatment. These results may provide important information on the impact of PEFs with sub-threshold intensities and durations on cell population growth and potential recurrence.

1. INTRODUCTION

Electricity and biology are inextricably connected. From ion channels in membranes to ion transport between the extracellular fluid and the cytoplasm, the movement of charged species plays a major role in cellular function. Thus, engineers and physicists frequently consider a cell as a multilayered dielectric with each layer (namely the plasma membrane, cytoplasm, nuclear envelope, and nucleoplasm) defined electrically by a permittivity (or capacitance) and conductivity (or resistivity). A eukaryotic cell containing a nucleus may thus be represented schematically, as in Fig. 1a [1-2], or as a circuit, as in Fig. 1b [3-4]. Each layer is therefore electrically defined by a capacitance that gives its charging time in the presence of an external electric field and a resistance that represents its ability to hinder ionic flow in the membranes or its concentration of ions in the cytoplasm or nucleoplasm.

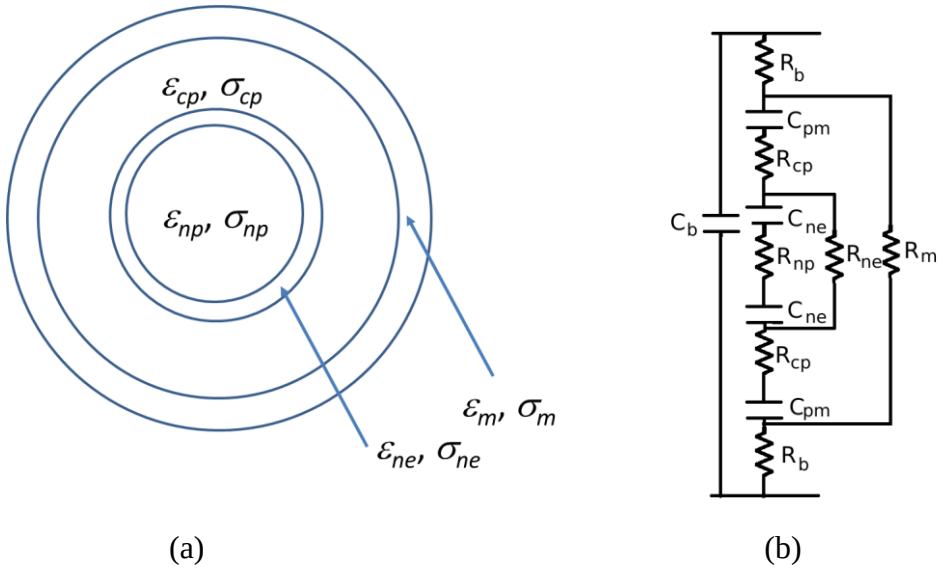

Fig 1. Electrical representation of the cell. (a) Multilayer dielectric representation of a cell [1] where ε and σ represent the permittivity and conductivity, respectively, of each layer, and *ne*, *np*, *cp*, and *m* represent the nuclear envelope, nucleoplasm, cytoplasm, and plasma membrane, respectively. (b) Circuit representation of a cell between two electrodes where *b* represents the extracellular (or buffer) solution, *pm* represents plasma membrane, and *R* and *C* are the resistance and capacitance of each layer, respectively [4].

1.1 Pulsed Electric Field Manipulation of Biological Cells

Given the importance of electrical properties in biological cells, it stands to reason that applying external electric fields to tissues and cells will induce functional and structural changes at the cellular, tissue, and organism levels. Pulsed electric fields (PEFs) above a certain intensity threshold can eradicate microorganisms [5-6]. Initially explained in terms of dielectric breakdown, charging the plasma membrane above a threshold voltage induced a rapid increase in membrane conductivity [7], subsequent experiments showed that PEFs of appropriate duration and field intensity induced temporary membrane permeabilization followed by cellular recovery [8]. This electropermeabilization can facilitate the cellular delivery of molecules normally unable to traverse the plasma membrane, paving the way for vaccine delivery, transdermal delivery [9], gene therapy [10], and electrochemotherapy [10-11].

The currently accepted mechanism for electropermeabilization is electroporation, or the formation of pores in the plasma membrane [12]. These pores arise when membrane voltages exceeding a few hundred millivolts alter the lipid bilayer [13]. Although incontrovertible experimental evidence of electroporation remains elusive, molecular dynamics (MD) simulations provide insight on the mechanism involved [14]. Through MD, Levine and Vernier showed that pore formation begins when an electric field induced a water defect into the bilayer interior [15]. Subsequent reorganization of the phospholipid head groups around the defect formed the pore with additional water and head groups migrating into the pore during pore maturation. Upon removing the electric field, the pore shrinks as the head groups and water vacate the membrane interior with membrane integrity restored once the head groups separate into two groups and all the water vacates the pore [15].

1.2 Nanosecond Pulsed Electric Fields

Conventional PEFs must be applied for a sufficient duration, typically on the order of hundreds of microseconds to a few milliseconds, to charge the cell membrane to induce sufficient membrane potential to permeabilize the cell membrane for electroporation. These pulses are my be square, exponentially decaying or Gaussian in shape with typical electric field strengths on the order of hundreds of V/cm to a few kV/cm. Applying similar total energies (which may be estimated by $Q = P/\tau$, where Q is energy, P is power, and τ is pulse duration with $P = IV = V^2/R =$

I^2R, where I is the current through the load, V is the electric potential drop through the load, and R is the resistance of the load, where the load is the cell suspension. To be completely correct, this must integrated with respect to time [102]) as these conventional electroporation PEFs over shorter durations of tens to hundreds of nanoseconds will not charge the membrane sufficiently to induce conventional membrane permeabilization in larger eukaryotic cells. Instead, these nanosecond duration PEFs (nsPEFs), which typically have pulse durations from 10-300 ns and electric field intensities from tens to hundreds of kV/cm, create nanopores on the outer cell membrane [16-18]. However, shorter duration of the nsPEFs is sufficient to fully charge the membranes of smaller intracellular structures such as the mitochondria, the membranes of vesicles to induce the release of intracellular calcium stores, or the nuclear envelope. Initial nsPEF experiments hypothesized that these nanosecond PEFs, nsPEFs, bypassed membrane effects to induce intracellular effects. These results were demonstrated in multiple ways with various mammalian cells. For instance, experiments showed that applying nsPEFs could induce apoptosis in certain cells without inducing permeabilization. Later experiments using electrical measurements [1] and the dye YO-PRO-1 [16-18] showed that nsPEFs induced pores of sufficient size to permit ions or small molecules to traverse the membrane, indicating the presence of nanopores smaller than those typical of conventional electroporation. These characteristics have paved the way for other applications of nsPEFs, such as platelet activation [19-21], which requires the permeabilization of membranes to facilitate Ca^{2+} entry to activate platelets and release the growth factors necessary for wound healing. In this thesis, the cytotoxicity of nsPEFs are explored for in vitro elimination of cancer cells.

Since bacteria are similar in size to the intracellular organelles, nsPEFs will be more likely to fully charge their membranes to induce pore formation. Chapter 2 of this thesis examines the combination of nsPEFs with various drug combinations to increase the cytotoxicity and effectiveness of gram-positive antibiotics on gram negative microbes, which may open a new pipeline for drugs to combat AMR. The ability to repurpose drugs that have already cleared the antibiotic regulatory pathways will provide additional options to healthcare personal for treating antibiotic resistant infections.

Chapter 3 investigates the impact of nsPEFs on the populations of E6 Jurkat cells, an acute T-cell leukemia suspension cell. The main focus of this Chapter is to extend previous experimental population studies to assess the applicability of a simple mathematical model for exploring the underlying biophysical behavior of the treated cell population due to a subthreshold PEF exposure,

which is important for in vivo studies where all cells may not be exposed to a uniform therapeutic PEF intensity. Characterizing the cancer cells as a population consisting of proliferating and quiescent cells, then further defining the transition rates to and from each with parameters for birth and death rates provides a framework to understand the effects of different pulse parameters to a single population over time. The limitations and conditions of the simple model are explained and appropriately fitted parameters.

2. ENHANCING GRAM POSITIVE ANTIBIOTIC EFFECTIVENESS ON GRAM NEGATIVE BACTERIA USING NANOSECOND ELECTRIC PULSES

This research was published (R. A. Vadlamani, A. Dhanabal, D. Detwiler, R. Pal, J. McCarthy, M. N. Seleem, and A. L. Garner, "Nanosecond electric pulses rapidly enhance the inactivation of Gram-negative bacteria using Gram-positive antibiotics," *Applied Microbiology and Biotechnology*, 104, 2217–2227 (2020).). R. A. Vadlamani and A. Dhanabal contributed equally to this work.

Reprinted by permission from Springer Nature: Applied Microbiology and Biotechnology, (Nanosecond electric pulses rapidly enhance the inactivation of Gram-negative bacteria using Gram-positive antibiotics, R. A. Vadlamani, A. Dhanabal, D. Detwiler, R. Pal, J. McCarthy, M. N. Seleem, and A. L. Garner), 2020. License Number 4814280288346.

2.1 Introduction

The discovery of antibiotics and their subsequent excessive or careless consumption has created antibiotic resistant pathogens, increasing the mortality rates from these infections and the cost burden on global healthcare systems [22]. Alexander Fleming expressed his concern of the population self-medicating inappropriately, either excessively or insufficiently [23], leading to the development of penicillin resistant microbes. The earliest pathogens resistant to penicillin arose within a decade of its discovery, and resistance mechanisms to various antibiotics can occur before completing their clinical trials or shortly after clinical use [22, 24-25]. Applying antibiotics in agriculture [26] and livestock farming [27] has further enhanced resistant pathogen development, potentially heralding the onset of the "post-antibiotic era" [28], where routine surgeries and simple scratches could lead to deadly infections reminiscent of the pre-antibiotic era. Antimicrobial resistance accounts for approximately 700,000 deaths annually, with predictions of 10 million deaths per year by 2050 [27]. The increased obsolescence of antibiotics, combined with the slow pace of new antibiotic development, especially in combating fluoroquinolone resistance in *P. aeruginosa*, has forced medical facilities to more frequently treat Gram-negative infections with older drugs, such as colistin, which are traditionally drugs of last resort and have more undesired side effects [27].

The pandemic nature of resistant plasmids and genes and the low economic return on investment for antibiotic discovery and development has discouraged pharmaceutical companies over the past two decades, leading to the dissipation of the antibiotic pipeline, especially for Gram-negative bacteria [24]. Gram-positive infections, such as methicillin-resistant *Staphylococcus aureus* (MRSA), comprise a significant portion of clinically relevant bacteria [27], and numerous novel antimicrobial drugs have been licensed to target them in the past decade [29]. While the list of essential medicines contains many drugs for combating Gram-positive infections [30], several of them, such as linezolid and vancomycin, have no clinically significant effect on most Gram-negative bacteria [31]. Even with public funding to incentivize new antibiotic development, such programs often require up to a decade to produce new molecules and compounds, and the nature of resistance mechanisms makes it likely that antibiotic resistance will develop more rapidly than new drug development. Thus, the current strategy of following a long and arduous process to develop new drugs followed by the rapid development of resistant microbes is one of escalating biological warfare.

This necessitates novel antimicrobial techniques. One approach entails repurposing drugs used for other medical treatments, such as arthritis, which exhibit antimicrobial properties [31-32]. Alternatively, one may combine drugs with different effects, such as one overcoming drug resistance mechanisms and the other inactivating the microbe by a common mechanism, such as inhibiting protein synthesis, nuclei acid synthesis, or cell wall synthesis. We previously achieved a similar result by combining nanosecond pulsed electric fields (nsPEFs) with antibiotics to inactivate microorganisms [33]. Other studies have examined electric fields for inactivating bacteria and biofilms for multiple applications [34], including sterilization [35] for wastewater treatment, food preservation and pasteurization [36-38], and biofilm removal from biomedical implants [39]. Electric fields can also enhance the susceptibility of biofilms and membranes to antibiotics [40], a concept that we extend to treat antibiotic resistant strains of bacteria.

We previously demonstrated that combining nsPEFs with antibiotics synergistically inactivates microbes [33]. In other words, combining trains of electric pulses (PEFs) and antibiotics, that were alone inadequate to induce clinically relevant microorganisms, could induce clinically significant microbe reduction (and in some cases complete sterilization) with a three to four minute nsPEF treatment time and ten-minute overall exposure time of the drug to the cells. This technique provides several advantages for treating antibiotic resistant mechanisms. First,

minimizing the drug dose and exposure time limits the possibility of creating resistance mechanisms. Second, the increased inactivation further reduces the likelihood of a surviving pathogen developing a resistance mechanism in that short time period. Finally, minimizing the exposure time could minimize any potential side effects to surrounding cells.

Another novel approach to combining nsPEFs with antibiotics involves leveraging the ability of PEFs to permeabilize microbial membranes to rapidly transport sufficient antibiotic levels into the microbe to overcome the antibiotic resistance mechanisms. While on the surface this may appear a subtle distinction, most studies combining PEFs to improve delivery of molecules or drugs, such as chemotherapeutics, into cells do so to enhance the delivery of a drug designed specifically to target the cell (or, at least, is highly cytotoxic). In this case, we propose to use the PEFs to permeabilize cells to make antibiotics that are normally ineffective at targeting a specific microorganism effective. Specifically, the relative abundance of Gram-positive antibiotics coupled with the dearth of Gram-negative antibiotics that can target resistant microorganisms motivated the current study. This study was designed to demonstrate the feasibility of using nsPEFs to render Gram-positive antibiotics effective against multiple species of resistant Gram-negative microorganisms.

2.2 Materials and Methods

2.2.1 Equipment:

A Blumlein pulse generator consisting of two lines comprised of twelve 2000 pF capacitors connected by inductors produced 300 ns PEFs with rise-times of 30 ns and fall-times of 35 ns at a repetition frequency of 1 Hz [41]. The PEFs were applied to a standard 2 mm gap electroporation cuvette (Dot Scientific ®) filled with a solution containing the microorganisms. We used a Luria broth of 0.5% salinity (5 g/L NaCl) for the solution to electrically match the resistance of the sample with the impedance of the pulse generator (11 Ω) to prevent signal reflection. The voltage measurements were taken using a LeCroy PPE 20 kV high voltage probe with a 1000:1 attenuation recorded by a TeleDyne LeCroy ® Waverunner 6 Zi Oscilloscope with a bandwidth of 4 GHz.

2.2.2 Sample Preparation:

These experiments combined nsPEFs with Gram-positive antibiotics to enhance the inactivation of two clinically relevant antibiotic resistant Gram-negative strains of bacteria and one

Gram-positive strain. The Gram-negative clinical isolates included a carbapenem-resistant *Escherichia coli* (ATCC® BA-2452™, New Delhi metallo-beta-lactamase NDM-1 positive, Carbepenem-resistant strain including imipenem and ertapenem) and a gentamicin, streptomycin and sulfonamide resistant *Pseudomonas aeruginosa* (BEI Resources NR-31040). We assessed the Gram-positive strain of methicillin resistant *Staphylococcus aureus* (MRSA USA300, a strain linked most frequently to skin infections in the United States), which is also resistant to erythromycin and tetracycline. Samples were cultured in Luria broth (LB Broth Lennox, powder microbial growth medium, SIGMA-ALDRICH ®) by taking 25 mL of broth in a 50 mL sterile conical tube and incubating in a shaker for 16 h at 37 °C. Samples were diluted 50 % by adding 25 mL media to the incubated sample as we plated controls for each experiment and condition.

The experiments assessed the following antibiotics: vancomycin, linezolid, rifampicin, mupirocin, erythromycin, and fusidic acid. Except for rifampicin, which has a broad spectrum of effectiveness against most Gram-positive and Gram-negative organisms, the five other antibiotics in this study primarily target Gram-positive bacteria and are largely ineffective or not used against Gram-negative bacteria in a clinical setting since they cannot effectively traverse their membranes [29][42]. Vancomycin is used primarily to treat Gram-positive bacteria such as MRSA, MRSE (methicillin resistant *Staphylococcus epidermis*), and other resistant strains of enterococci. Linezolid is used primarily against Gram-positive bacteria such as MRSA, vancomycin resistant enterococci and streptococci. Mupirocin is used primarily to treat MRSA and other *S. aureus* strains, with mupirocin resistant *S. aureus.* arising almost immediately after clinical trials. Although its mechanism is incompletely understood, erythromycin is bacteriostatic and acts internally by binding to the 50s subunit of the rRNA complex and is also used primarily against Gram-positive bacteria. Fusidic acid is another bacteriostatic compound used primarily to treat Gram-positive bacteria with MRSA and *S. aureus* strains exhibiting resistance. Of the antibiotics studied here, the WHO Model list of essential medicines includes rifampicin and vancomycin and classifies linezolid as a drug of last resort [30].

2.2.3 Electric Pulse Treatment Protocol:

Samples were treated in 2 mm gap cuvettes containing 365 µL of sample between the electrodes, with bio-grade mineral oil added on top of the electrodes to prevent arcing. PEF treatments in previous studies [34], [43] examined the effect of electric fields on microbial

inactivation, while recent studies [33] assessed the synergistic combination of nsPEFs and antibiotics. This study used similar nsPEF parameters as our previous study [33], which started with low electric fields and antibiotic dosages that induced minimal inactivation alone, but showed significant inactivation when combined. These results were compared to a higher electric field capable of inactivating bacteria independently with varying effectiveness across strains. We then assessed the improvement in inactivation introduced by adding the antibiotics to these PEFs.

To establish a common baseline for comparing different nsPEF parameters, we fixed the energy density U delivered to the cuvettes according to

$$U = NE^2\tau, \tag{1}$$

where N is the number of pulses and τ is the pulse duration [44]. We applied either 500 300 ns PEFs at 20 kV/cm or 222 300 ns PEFs at 30 kV/cm to deliver equivalent energy to the sample. Figure 1 shows a representative waveform for each PEF intensity with the electric field $E = V/D$, with V the measured applied voltage and D the cuvette gap distance.

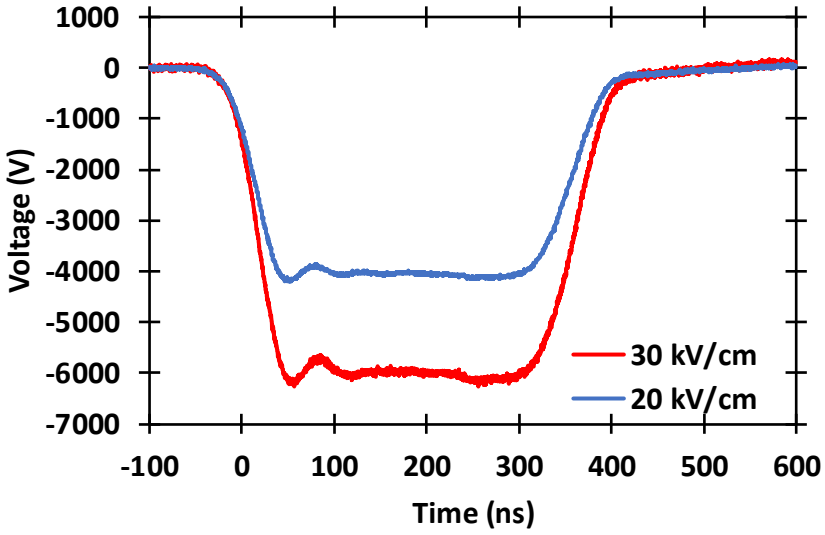

Figure 1: Representative waveforms for the 20 kV/cm and 30 kV/cm 300 ns electric pulses with applied electric field E = V/D, where V is the measured voltage and D is the cuvette gap distance.

2.2.4 Plating:

Tissue culture Petri dishes from VWR ® (15 cm diameter, 10 mm height) were utilized for plating. Each plate was covered with 15 mL of Luria broth (Agar, microbiology tested powder, SIGMA-ALDRICH ®), which was prepared by adding 20 g of LB Lennox (SIGMA-ALDRICH) and 15 g/L of agar to water prior to being autoclaved. The salinity of the agar was the same as the LB (0.5% NaCl) to minimize additional environmental stressors on the bacteria.

We removed 20 µL from each cuvette and added it to 180 µL of PBS in a 96-well dish in triplicate. Each well was then diluted by a ratio of 10:1 five additional times by taking 20 µL of the diluted sample into subsequent wells using multi-channel pipettes (using fresh tips for each dilution). We plated the six dilutions of each sample two times each by adding 4 µL from each well onto the Petri dish using a multi-channel pipette, which allowed the plating of all three replicates on the same plate to then averaged to find the final concentration. These plates were then cultured overnight in an incubator at 37 °C and counted the next day. We performed at least three replicates for each condition.

Counts were taken for relevant dilutions (colony counts ranged from 15 to 25 colonies) and multiplied by $25\times10^{\text{dilution}}$, to account for the 4 µL plated for each condition. These experiments were repeated three times each over different days with different incubated samples.

2.2.5 Statistical Analysis:

A two-way ANOVA (alpha = 0.05) was run to determine the statistical significance of the log reduction from drug and field treatments. Performing a Dunnett's multiple comparison test in addition to the ANOVA permitted us to compare the different concentrations of each drug at each field intensity. Results are presented as *p*-values and significant differences from the Dunnett's test are marked appropriately in the figures.

2.3 Results and Discussion

2.3.1 Bacterial inactivation combining Electric Pulses (PEFs) with antibiotics

We assessed various combinations of the antibiotics above with nsPEFs for inactivating one Gram-positive and two Gram-negative bacteria. Table 1 summarizes the ANOVA assessment of the various treatments to assess the statistical significance of adding 2 or 20 µg/mL with or

without PEFs. All drugs except fusidic acid had significant effects on *E. coli* inactivation. For *P. aeruginosa*, rifampicin is the only drug that had a significant effect, indicating that the Gram-positive drugs remained ineffective against this Gram-negative strain. Combining mupirocin and rifampicin with PEFs significantly improved the inactivation of the Gram-positive strain MRSA compared to PEFs alone.

Table 1:ANOVA p-values for antibiotic effectiveness on bacterial inactivation compared to either no PEF treatment or PEF treatment without antibiotics. Bold values are significant ($p < 0.05$).

Drug	**MRSA**	***E. coli***	***P. aeruginosa***
Linezolid	0.3349	**0.0076**	0.2915
Fusidic acid	0.8543	0.15	
Erythromycin	0.771	**0.0088**	0.1559
Mupirocin	**0.03**	**<0.0001**	0.1559
Rifampicin	**0.0009**	**<0.0001**	**0.0288**
Vancomycin	0.588	**0.0021**	0.1888

Table 2 shows our application of Dunnett's test to compare 2 and 20 µg/ml doses to no drug concentration to further elucidate PEF-enhancement of drug effectiveness and specifically assess whether further increasing drug concentration enhances inactivation. These results are also evident in Figures 1-3 for each individual microorganism.

Table 2: Dunnett's comparison of the statistical significance of 2 and 20 µg/mL of each drug to the no drug treatment following no pulsed electric field (PEF) exposure and treatment with either 500 20 kV/cm or 222 30 kV/cm 300 ns PEFs. Significant values ($p < 0$) are bolded.

Drug	Electric Field (kV/cm)	Concentration Compared to no Drug (µg/mL)	MRSA	*E. coli*	*P. aeruginosa*
Linezolid	0	2	0.9891	0.9956	0.9476
		20	0.9891	0.9956	0.8715
	20	2	0.8759	**0.0209**	0.9891
		20	0.9972	**0.0041**	0.3510
	30	2	0.2234	0.0617	0.7909
		20	**0.0371**	0.1246	**0.0011**
Fusidic acid	0	2	0.9912	0.9990	
		20	0.9601	0.9997	
	20	2	0.9762	0.7310	
		20	0.7844	0.5057	
	30	2	0.3935	0.1076	
		20	0.2754	0.0647	
Erythromycin	0	2	0.9383	0.9936	**0.0138**
		20	0.9841	0.7533	0.8956
	20	2	0.8253	0.1154	0.9681
		20	0.9960	0.6584	0.6966
	30	2	0.5644	**0.0097**	0.2143
		20	0.4251	**0.0002**	0.3124
Mupirocin	0	2	0.9773	0.9871	0.6583
		20	0.9974	0.9497	0.8970
	20	2	0.9772	**0.0093**	0.7885
		20	0.5447	**0.0123**	0.9812
	30	2	0.3875	**<0.0001**	0.0534
		20	**0.0015**	**0.0003**	0.2321
Rifampicin	0	2	0.5859	0.9573	0.9947
		20	0.4717	0.9891	0.4850
	20	2	**0.0086**	**0.0342**	0.9528
		20	0.3090	**<0.0001**	0.3603
	30	2	**0.0311**	**0.0001**	**0.0087**
		20	**0.0015**	**<0.0001**	**0.0029**
Vancomycin	0	2	0.9900	0.9196	0.9908
		20	0.9777	0.9537	0.6618
	20	2	0.9899	0.5812	0.7648
		20	0.9899	0.1002	0.7964
	30	2	0.3019	**0.0390**	0.5665
		20	0.1851	**0.0003**	0.1245

Figure 2 highlights the inactivation of MRSA USA300 under these conditions and the resulting improvement due to adding a single antibiotic to the nsPEFs. Treating MRSA USA300 with either 2 μg/mL or 20 μg/mL of any of the drugs alone induced less than 1-$\log_{10}$ reduction. Applying either 500 20 kV/cm or 222 30 kV/cm 300 ns PEFs with no drugs induced over 1.5-$\log_{10}$ or 4-$\log_{10}$ reduction, respectively. Since these nsPEFs had the same pulse duration and delivered the same overall energy density to the microbes, and the time between PEFs of 1 s is sufficient for many pores to reseal [45], this suggests that the higher electric field has a dramatic and statistically significant ($p < 0.0001$) effect on MRSA USA300 inactivation compared to the lower electric field. With all else equal, raising the electric field increases the membrane potential, making both reversible and irreversible electroporation more likely. Because only very long-lived pores will remain for either nsPEF condition, the driving factor for membrane level effects will likely be the increased membrane potential and subsequent pore formation from a single nsPEF, suggesting that the 30 kV/cm should have the larger impact.

Figure 2 shows that combining certain concentrations of specific drugs with PEFs can induce a statistically significant improvement in inactivation efficacy compared to applying PEFs alone. For instance, adding 2 or 20 μg/mL of rifampicin with 30 kV/cm PEFs, 2 μg/mL of rifampicin with 20 kV/cm PEFs, 20 μg/mL of linezolid with 30 kV/cm PEFs, or 20 μg/mL of mupirocin with 30 kV/cm PEFs induced a statistically significant increase in microorganism inactivation compared to the corresponding PEF with no drug. This suggests that the improved permeabilization of these nsPEFs plays a critical role in enhancing the efficacy of these specific drugs for inactivating MRSA USA300. Since all the drugs except for rifampicin specifically target Gram-positive microorganisms, incorporating these levels of nsPEFs to facilitate their entry into MRSA does not statistically significantly improve the efficacy compared to nsPEFs alone. The ability to improve nsPEF efficacy by incorporating a small level of rifampicin could be valuable in cases necessitating broad spectrum antibiotics since treatments usually attempt to avoid over-reliance on rifampicin to mitigate the risk of the development of antibiotic resistance [46-47]. Moreover, since combinations of rifampicin and fusidic acid are often used to treat MRSA, particularly for prosthetic joint infections [47], this result could have practical clinical application for localized infections.

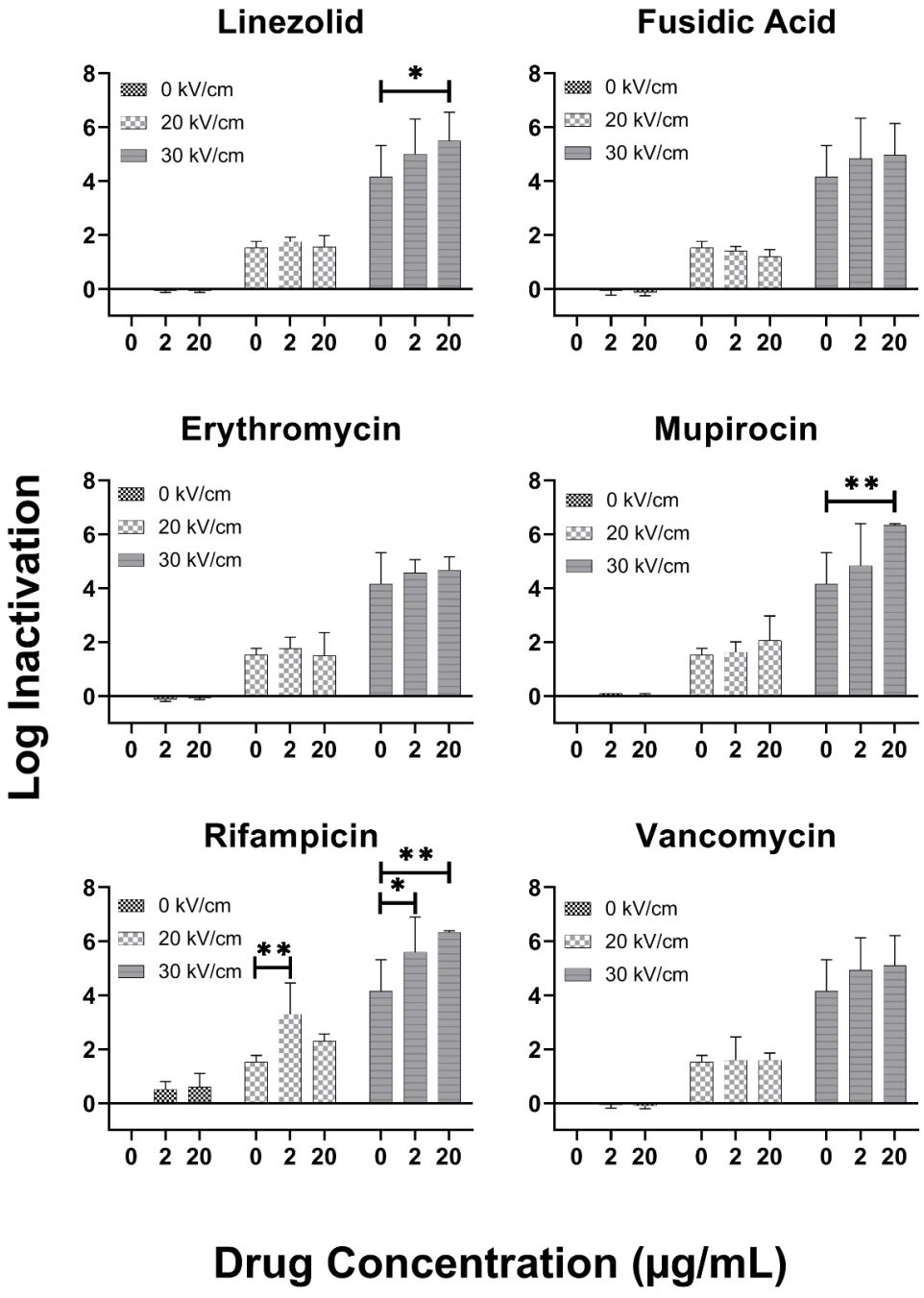

Figure 2: Inactivation of MRSA USA300 following treatment with 300 ns electric pulses (PEFs, 500 at 20 kV/cm and 222 at 30 kV/cm) and/or various concentrations of antibiotics. Adding 2 or 20 µg/mL of rifampicin with 30 kV/cm PEFs, 2 µg/mL of rifampicin with 20 kV/cm PEFs, 20 µg/mL of linezolid with 30 kV/cm PEFs, or 20 µg/mL of mupirocin with 30 kV/cm PEFs induced a statistically significant increase in microorganism inactivation compared to the corresponding with no drug. The error bars are determined from standard deviation. Significant differences in inactivation at each electric field intensity are denoted as follows: * $p < 0.05$; **$p < 0.01$.

2.3.2 Inactivating Gram-negative bacteria with Gram positive antibiotics

Figure 3 shows the inactivation of Gram-negative *E. coli* by Gram-positive antibiotics. Applying 2 μg/mL or 20 μg/mL of linezolid, fusidic acid, erythromycin, mupirocin, rifampicin, or vancomycin induced no statistically significant changes in *E. coli* population, relative to untreated control. Applying the 20 or 30 kV/cm nsPEFs induced a statistically significant 1.5-$\log_{10}$ or 2.6-$\log_{10}$ inactivation ($p < 0.0001$), respectively.

Combining the 20 or 30 kV/cm nsPEFs with 2 μg/mL or 20 μg/mL of rifampicin or mupirocin induced statistically significant increases in microorganism inactivation, indicating that the nsPEF induced membrane permeabilization enhances the efficacy of these antibiotics. Specifically, applying 2 or 20 μg/mL of rifampicin with 20 kV/cm PEFs resulted in an additional 0.7 and 1.6-$\log_{10}$ reduction, respectively, compared to PEFs alone and 1.5 and 3.6-$\log_{10}$ reduction, respectively, compared to 30 kV/cm PEFs. Combining the 30 kV/cm PEFs with 20 μg/mL of rifampicin resulted in over 6.1-$\log_{10}$ reduction, which was the highest of any combination studied. Adding 2 or 20 μg/mL of mupirocin with 20 kV/cm PEFs led to approximately 0.8-$\log_{10}$ additional inactivation compared to the PEFs alone. Adding 2 or 20 μg/mL of mupirocin with the 30 kV/cm PEFs enhanced inactivation by 1.8- or 1.232-$\log_{10}$, respectively, compared to the PEFs alone.

Combining 2 or 20 μg/mL of vancomycin or erythromycin with the 20 kV/cm PEFs did not improve inactivation efficacy; however, combining either concentration of these antibiotics with the 30 kV/cm PEFs did improve *E. coli* inactivation. Specifically, combining 2 or 20 μg/mL of erythromycin with the 30 kV/cm PEFs improved inactivation by 1-$\log_{10}$ and 1.6-$\log_{10}$, respectively, compared to the 30 kV/cm PEFs alone. Combining 2 or 20 μg/mL of vancomycin with the 30 kV/cm PEFs enhanced inactivation by 1 and 2.1-$\log_{10}$, respectively, compared to the PEFs alone. The peak inactivation of 4.4-$\log_{10}$ and 4.6-$\log_{10}$ for erythromycin and vancomycin, respectively, occurred when combining 20 μg/mL of each antibiotic with the 30 kV/cm PEFs.

For linezolid, combining 2 or 20 μg/mL of the antibiotic with the 20 kV/cm PEFs resulted increased the inactivation by 1.268- or 1.601-$\log_{10}$, respectively, compared to the PEFs alone to an overall inactivation of 3-$\log_{10}$. Combining either concentration of linezolid with the 30 kV/cm PEFs improved inactivation by approximately 1-$\log_{10}$ compared to the PEFs alone for a total inactivation of 3.6-$\log_{10}$; however, this improvement was statistically insignificant compared to the 30 kV/cm PEFs. Thus, both the enhanced inactivation induced by linezolid compared to the

nsPEFs alone and the overall inactivation was smaller than the peak levels of rifampicin, mupirocin, vancomycin, and erythromycin.

Combining either 2 or 20 μg/mL of fusidic acid with 20 kV/cm PEFs did not induce a statistically significant change in inactivation compared to the PEFs alone. Combining 2 or 20 μg/mL of fusidic acid with the 30 kV/cm PEFs induced a 1.383- or 1.566-$\log_{10}$ improvement in inactivation compared to the PEFs alone, respectively, for an overall inactivation of 4.1-$\log_{10}$; however, the improvement was not statistically significant compared to the PEFs alone.

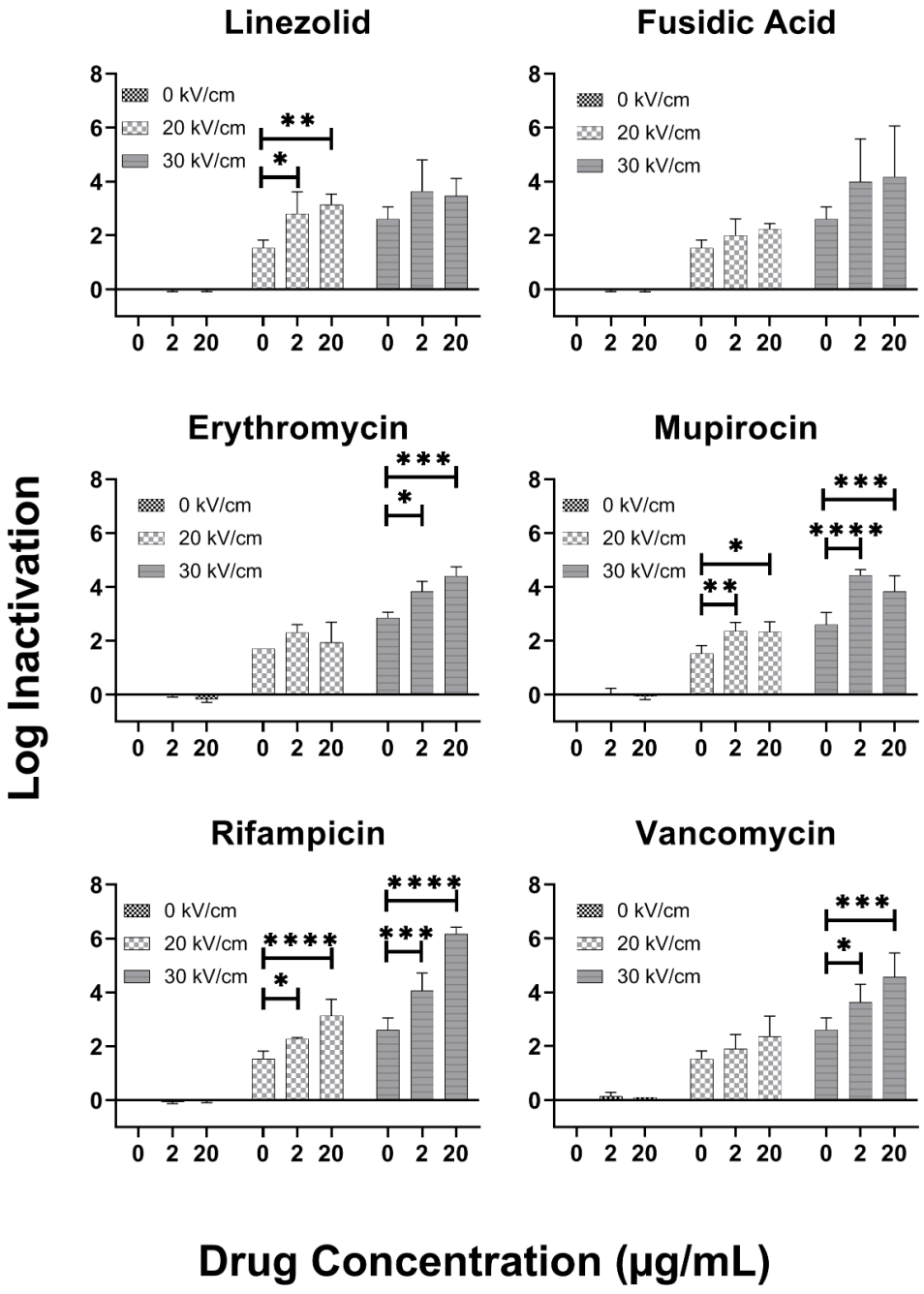

Figure 3: Inactivation of E. *coli* following treatment with 300 ns electric pulses (PEFs, 500 at 20 kV/cm and 222 at 30 kV/cm) and/or various concentrations of antibiotics. The error bars are determined from standard deviation. Significant differences in inactivation at each field intensity are marked as follows: *p < 0.05; **p < 0.01; ***p < 0.001; ****p < 0.0001. The increased membrane permeabilization induced by the PEFs increased the inactivation for both drug concentrations and PEF intensities for rifampicin and mupirocin, for the higher PEF intensity for erythromycin and vancomycin, and for the lower PEF intensity for linezolid.

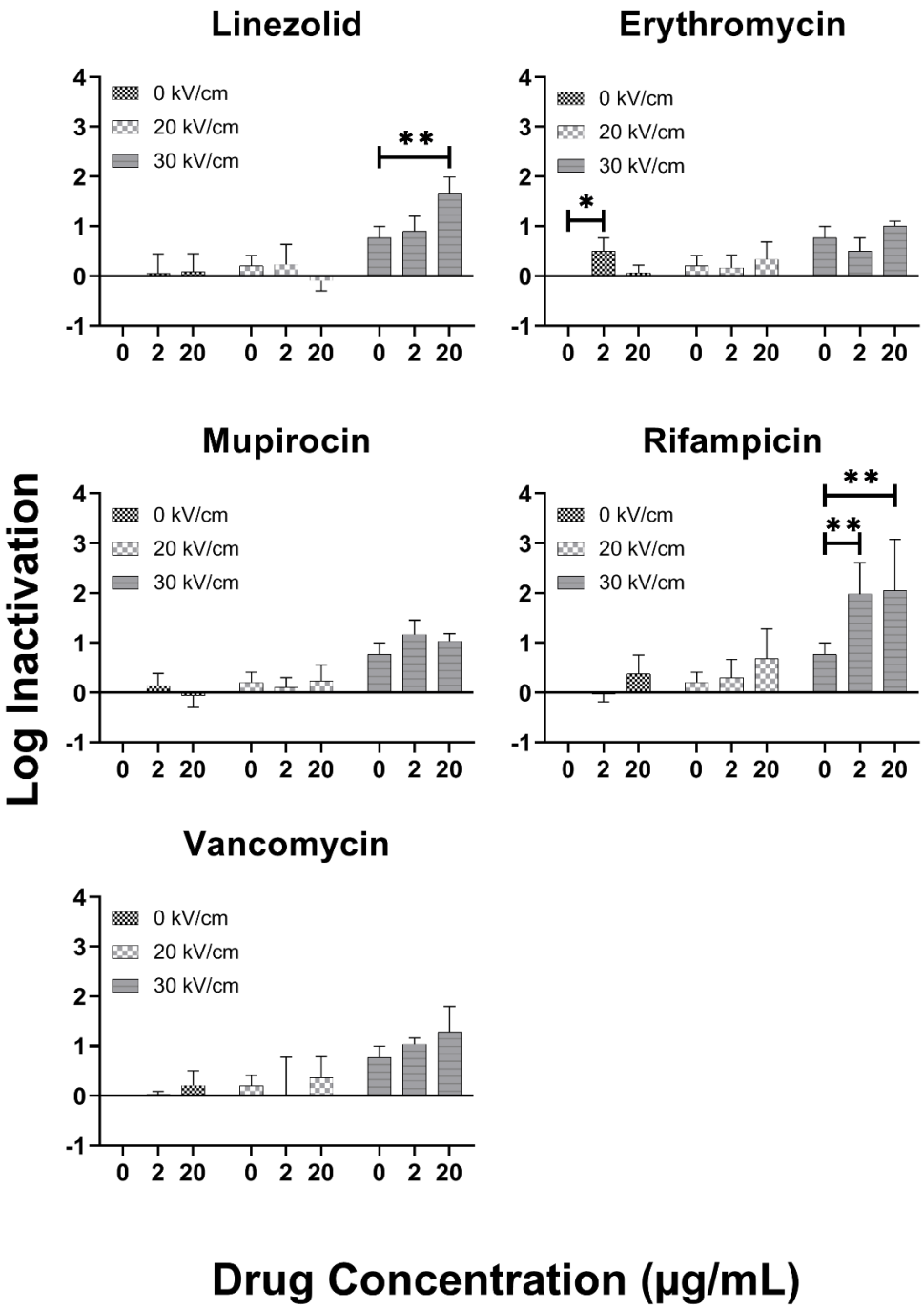

Figure 4: Inactivation of P. *aeruginosa* following treatment with 300 ns electric pulses (PEFs, 500 at 20 kV/cm and 222 at 30 kV/cm) and/or various concentrations of antibiotics. Adding 20 µg/mL of linezolid or 2 or 20 µg/mL of rifampicin to the 30 kV/cm PEF train induces a statistically significant increase in inactivation compared to the PEFs themselves. The error bars are determined from standard deviation. Significant differences in inactivation at each field intensity are marked as follows: *$p < 0.05$; **$p < 0.01$.

For *P. aeruginosa*, a biofilm forming bacteria, Figure 4 shows that the drugs alone induced no activation, the 20 kV/cm nsPEFs induced approximately 0.2-$\log_{10}$ reduction, and the 30 kV/cm nsPEFs induced 0.8-$\log_{10}$ reduction. In this case, combining 20 μg/mL of linezolid to the 30 kV/cm PEF train induced a statistically significant increase of approximately 0.9-$\log_{10}$ of inactivation compared to the PEFs alone for a total of 1.7- $\log_{10}$ inactivation. Adding 2 or 20 μg/mL of rifampicin to the 30 kV/cm PEF train led to a statistically significant 1.211- or 1.282- $\log_{10}$ increase in inactivation compared to the PEFs alone, respectively for a total of 2-$\log_{10}$ inactivation. No other drug concentrations resulted in a statistically significant increase in inactivation compared to the PEF trains alone. Adding 2 μg/mL of erythromycin alone induced a statistically significant inactivation of 0.5 $\log_{10}$ inactivation without PEF trains.

2.4 Implications and Conclusion

Previous studies have established the ability of nsPEFs to inactivate bacteria [34][48-49] and demonstrated a synergistic effect of nsPEFs on the effectiveness of antibiotics [33] to inactivate both Gram-positive and Gram-negative bacteria or natural ingredients [50-51] to inactivate Gram-negative bacteria. The growing threat of antibiotic resistant infections combined with a lack of drugs in the discovery pipeline necessitates the exploration for novel ways to enhance the effectiveness of existing antibiotics to treat these infections. nsPEFs may provide a means to make Gram-positive antibiotics, which are abundant, effective against Gram-negative resistant strains of bacteria, for which new and effective medicines are sorely lacking, while accomplishing this on a sufficiently short timeframe to prevent resistance mechanisms from developing (due to long exposure times, allowing the bacteria to evolve under antibiotic pressure).

The statistically significant levels of inactivation for certain combinations of Gram-positive antibiotics and PEFs on both Gram-positive and Gram-negative bacteria compared to PEFs alone indicates that the antibiotics can enhance inactivation due to the PEFs facilitating the antibiotics' ability to reach their targets inside the bacteria. Of particular note, combining certain concentrations of rifampicin, vancomycin, mupirocin, erythromycin, and linezolid with different trains of PEFs induced a statistically significant increase in *E. coli* inactivation compared to the PEFs alone, indicating that PEFs overcome the resistance mechanisms that prevent these antibiotics from acting. This could enable the repurposing of these antibiotics toward treating Gram-negative bacteria and minimize the need to design new Gram-negative antibiotics. Further

tuning PEF duration, electric field, number of PEFs, or repetition rate may improve the synergistic inactivation antibiotics. Traditionally, scientists tune PEF parameters to modify the plasma membrane potential V_m. Inducing $V_m \gtrsim 250$ mV for sufficient duration [13] generates sufficient membrane pores to transport molecules across the membrane. However, PEFs also induce temperature changes and temperature gradients that facilitate membrane permeabilization and ion and molecular transport [52-54]. Thus, adjusting PEF parameters may not only enhance electro permeabilization by increasing V_m, but induce other physical mechanisms that may provide additional positive feedback to facilitate antibiotic delivery and enhance inactivation.

It is difficult to inactivate *P. aeruginosa* with these PEF parameters except in combination with rifampicin and, even then, the inactivation levels are much lower than for *E. coli*. This could necessitate using longer duration PEFs, higher electric fields, or longer overall exposure times than studied here. It may also necessitate combining with other potentially helpful phenomena, such as increasing temperature. Thus, future studies may additionally explore additional optimization of the treatment approach. Since targeted microorganisms or clinically relevant conditions may vary, such as treating the surface of a wet wound or treating an implant, a flexible pulsed power architecture that permits treating various electrical impedances and modify PEF parameters [55] across pulse durations may be valuable. Moreover, or exploration of bipolar waveforms may enhance treatment efficacy for millisecond duration PEFs [56].

As alluded to in previous nsPEF studies [33], the present approach would be useful for treating localized infections, such as at a surgical site, wound, or implant, and not for treating systemic infections. Since many systemic infections have their origin from localized infections during surgery or due to a wound, this approach could mitigate the risk of subsequent infection by inactivating microorganisms prior to the infection becoming systemic. Moreover, nsPEFs provide an advantage over other inactivation techniques, such as cold atmospheric pressure plasmas (CAPPs) [57], for treating wounds because the liquid present in the wound actually provide a medium for delivery rather than an impediment for reactive species transport for inactivation in the case of CAPPs.

In summary, these in vitro results demonstrate that combining Gram-positive antibiotics with nsPEFs can enhance the inactivation of *E. coli* compared to nsPEFs alone, but only very slightly for *P. aeruginosa*. Future studies exploring treatment mechanism and PEF parameter

optimization will further elucidate the potential clinical application of this approach for localized infection treatment.

3. MODELLING CANCER CELL POPULATION DYNAMICS WITH NANOSECOND PULSED ELECTRIC FIELDS

This Chapter extends prior work presented in a prior dissertation [58] in the research group. This prior work assessed the behavior of the number of Jurkat cells, an immortalized T-cell leukemia cell line, to various pulsed electric fields (PEFs). Part of this work attempted to fit these results to a mathematical theory, but with limited success. This thesis completes this effort and demonstrates the conditions under which this theory may be applied. Some of the background and methods come from this prior dissertation.

3.1 Introduction

Cancer cell populations contain proliferating, quiescent, and dead cells that drive tumor growth and cancer metastasis based on the surrounding microenvironment [59-62]. Effective cancer treatments often target the proliferating cells [63-66], which simplified population models show will ultimately eradicate the cancer cell population if the transition from quiescent to proliferating is sufficiently small [61]. Thus, characterizing the transition between these states is critical for understanding treatment effectiveness. One way to do this is by mathematically modeling the cell population as a combination proliferating cells and quiescent cells, as shown in Fig. 3.1. More details on this model will be provided in Section 3.2.

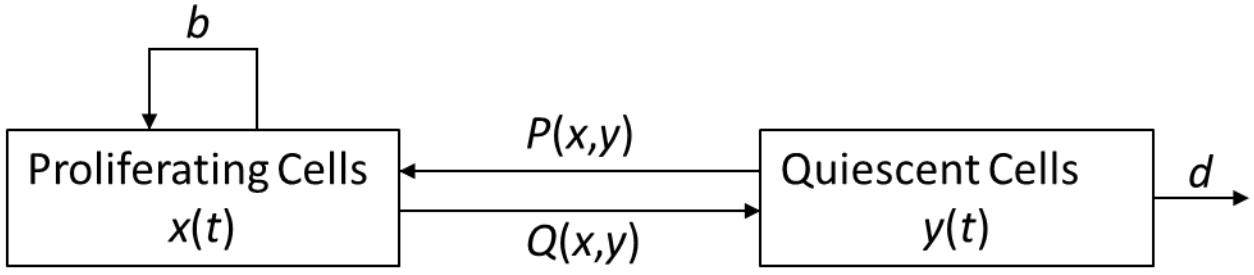

Figure 5: Schematic representing a simple mathematical model for cancer cell population dynamics assuming that it is comprised of proliferating cells $x(t)$ and quiescent cells $y(t)$ that vary as functions of time t. The proliferating cells divide at a rate b and transition to the quiescent state at a rate $P(x,y)$. The quiescent cells transition to the proliferating state at a rate $Q(x,y)$ and die at a rate d. Typically, $Q(x,y) << P(x,y)$.

The transition between cell division states becomes particularly important for cancer stem cells (CSCs), which are a small subpopulation of abnormal cells that maintain and drive tumor growth for multiple cancer types and are thus an important target in cancer treatment [67]. Because they may remain quiescent for extended periods of time, making them less susceptible to treatments for proliferating cells [69-72], and their metabolism strongly resembles other cells [67-68], eradicating CSCs remains a tough clinical challenge. In this state, CSCs exhibit great "robustness," characterized by a long cell cycle (thus appearing quiescent), the ability to detoxify or mediate cytotoxic agents (including pumping out drugs), resistance to oxidative stress, and responsiveness to DNA damage [63], [68]. CSCs may also ultimately recruit blood vessels and metastasize [69].

Thus, effective cancer treatments must simultaneously eradicate the proliferating cells responsible for tumor growth and cancer spread while additionally impacting the quiescent, or dormant, cells that may eventually induce a relapse. Since the dormancy of CSCs makes targeting them with traditional treatments challenging, one alternative strategy involves targeting their quiescence [68]. For instance, chronic myeloid leukemia (CML) is often treated with imatinib, which targets the oncogenic fusion protein produced by the Philadelphia chromosome [73]; however, imatinib strongly inhibited differentiated leukemia cells, while not depleting the stem cells [74]. Ablating Fbw7, an antimetastatic protein, can successfully make imatinib-resistant CML cells sensitive to the drug again [68]. Thus, one may control cell cycle as a means to effectively treat cancer.

Nanosecond PEFs (nsPEFs), with durations from 10-300 ns and electric fields from ~30 kV/cm to 300 kV/cm, may also interact with biological cells [4]. While nsPEFs may create nanopores in the plasma membrane [75], they may also manipulate intracellular structures, such as the mitochondria, since they fully charge these smaller structures before the plasma membrane [76]. These nsPEFs have effectively induced apoptosis in melanomas [24] and have since been used for basal cell carcinoma (BCC) therapy [77] and breast cancer treatment [78] in humans. They also cause pyknosis of the nuclei in the BCC while also inducing the endoplasmic reticulum to release the protein calreticulin [77]. When calreticulin is trapped in the lipid bilayer, it signals the dendritic T-cells that the apoptotic pathway has been opened [77].

The importance and utility of different PEFs for treating cancer and the importance of targeting populations of both proliferating and quiescent cells for an effective treatment motivates better understanding the impact of PEFs on cancer cell population dynamics. This is particularly critical since PEFs may selectively target different cells [79] and lower strength electric fields may actually increase cell growth [80]. In fact, even for tumor treatment, although PEFs may initially destroy a small fraction of the cancer cell population, the total cell population may actually increase over time [25].

Another promising alternative PEF approach is electrochemotherapy [81]. The utilization of nsPEFs in this approach fixate on tumor regions without excessive heating, essentially permitting exposure of toxic drugs into the cancer cells as a result of electropermeabilization. Electrochemotherapy can be used minimally and effectively towards a single target region for the eradication of tumors through nsPEFs. The importance of nsPEF in electrochemotherapy can be emphasized in the lack of thermal ablation causing necrosis of tissue and the direct poration of cancer cell membranes. In actuality, nsPEFs typically affect the tissue in the area of the delivery electrode whilst inhibiting tumor blood flow to prevent metastasis.

The nanosecond pulsed electric fields have been proven to serve as effective candidates [82] in cancer therapy, mainly as a mechanism directly targeting intracellular structures, surrounding vasculature, and the plasma membrane.

Recent studies have demonstrated the utility of nsPEFs for in vivo tumor treatment [83]. In on example, nsPEFs induced cell apoptosis in pancreatic carcinoma through the intrinsic pathway (mitochondrial-dependent). In other cases, nsPEFs can target the mitochondrial membrane potentials leading to a BcL-2 protein imbalance [84]. In the same microenvironment, the cell proliferation function in the NF-kB signaling pathway was disrupted through the repression of cyclin proteins responsible for transcriptional activity of DNA. A critical aspect to this study was the inhibition of metastasis by suppression of the Wnt/β-Catenin signaling pathway, which directly inhibits cell proliferation and cell migration. The nsPEFs involved in disrupting cancer growth in these targeted areas reveal extensive biological effects and warrant further study in the PEF parameters required to trigger apoptotic responses [85].

Thus, this chapter explores the impact of various numbers and intensities of 60 ns and 300 ns PEFs on E6 Jurkat cells, an acute T-cell leukemia suspension cell line found in the peripheral blood of tissues as a result of acute T-cell leukemia. This chapter extends work reported in a

previous dissertation by another member of the research group [58] and determines the relevant conditions for which the mathematical model is valid. Specifically, this chapter shows that the model is relevant when the cell population continues to increase following treatment, exhibiting an S-curve (logistic) behavior similar to untreated population growth. The critical difference between the treated and the untreated cell populations is the final steady state behavior. The mathematical model under the treatment conditions can elucidate the impact of PEF parameters on cell population behavior and provide valuable information about sub-threshold fields on long-term cancer cell survival. This can provide valuable information for clinical applications where, despite best efforts, the PEF exposures to tumors will be nonuniform, causing some cells to undergo sub-threshold fields. The application of the simple theory reported here provides some preliminary insight into the behavior of cells following sub-threshold treatment in vitro that may ultimately be extended for studies in in vivo environments.

Section 3.2 will outline the equipment, procedure, and mathematical model used in this study. Section 3.3 summarizes the experimental results and the parameters that arise from fitting the model. We discuss the implications of the results in Section 3.4 and make concluding remarks in Section 3.5.

3.2 Materials and Methods

3.2.1 Pulsed Power Equipment

As described previously [58], this study used 300 ns and 60 ns Blumlein pulse generators designed to terminate into an 11 Ω and 20 Ω load, respectively, with a pulse repetition frequency of 1 Hz and triggered using a brass spark gap switch. The 300 ns Blumlein pulse generator was charged by twenty-four 40 kV capacitors and twenty-four 600 nH inductors. The 60 ns pulse generator was a two-stage Blumlein consisting of RG-213 transmission lines. We applied PEFs from the generators into 2 mm gap cuvettes (Biorad®) containing the cell suspension.

We measured the applied voltage using a high voltage probe of 1000:1 attenuation (LeCroy 100 MHz, 20 kV model PPE20KV) connected to a Waverunner 6 Zi Oscilloscope (TeleDyne LeCroy®). We report the applied electric field as $E = V/d$, where V is the peak voltage of the applied pulse and d is the gap distance. Fig. 6 shows representative waveforms for each pulse

generator with the 60s ns pulse generator duration taken as the full width at half maximum (FWHM) and the 300 ns pulse generator duration taken at the peak.

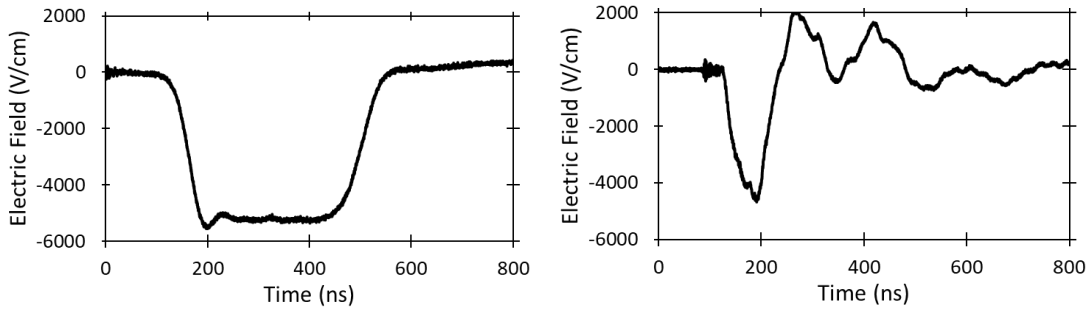

Figure 6: Representative waveforms for 300 ns (left) and 60 ns (right) electric pulses.

3.2.2 Cell Suspension Preparation.

Cells were cultured in RPMI 1640 (Gibco™) containing 1% antibiotics (penicillin-streptomycin) and 10% fetal bovine serum (FBS) and 5 mM L-Glutamine in 10 cm cell culture treated Petri dishes (VWR ®) in a 5% CO_2 incubator at 37°C. The 0.5% salinity of the growth media provides the ideal conductivity to electrically match the cuvettes to the pulse generator's 11 Ω output impedance. This experiment used Jurkat, Clone E6-1 cells (ATCC ®), an immortalized acute T-cell leukemia suspension cell line. The cells were preserved in liquid nitrogen and thawed in a 37°C water bath, centrifuged to remove the supernatant and then suspended in RPMI-1640 growth media. The cells were passaged upon reaching 90% confluency, between 60 and 72 hours (approximately 3×10^6 cells/ml), with fresh media added for every third passage by centrifuging, draining supernatant, and resuspending the pellet in fresh media to drain away detritus, with plating for each passage plated at 5×10^5 cells/ml. To maximize consistency between experiments, samples were tested between the eighth and twenty-fifth passages.

3.2.3 Electric Pulse Treatment Protocol

Cells were placed in 2 mm cuvettes, filled with 410 µL of the sample diluted to a concentration of 2×10^6 cells/ml as determined using a Countess II ® Automated Cell counter (confirmed initially using a hemocytometer), and pulsed using clinically relevant parameters [24]. The cuvettes were pulsed at a repetition rate of 1 Hz to minimize potential effects from multiple pulses at high repetitions rates [86] such membrane sensitization and temperature effects, including sample heating and localized temperature gradients, which may facilitate membrane permeabilization [87].

We applied trains of ten, thirty and fifty 300 ns PEFs at 5 kV/cm, 20 kV/cm and 30 kV/cm to assess the impact of applied electric field. To assess the effect of pulse duration, we applied 360s PEFs such that the applied energy, determined by,

$$U = NE^2\tau \quad (1)$$

was the same as 5 kV/cm, 300 ns PEFs. We counted the cells immediately post pulsing by using a 50% by volume Trypan Blue mix with the disposable slides for the Countess to determine the immediate kill – off due to pulsing. Each experiment had 3 different parameters along with a control that were performed, entailing 4 different conditions in 12 wells, totaling 3 replicates per condition.

3.2.4 Plating/Counting

Counts were taken every twelve hours with samples spun down and media exchanged every twenty-four hours. Unlike previous studies [88], we fed our samples with additional nutrients during the study to more closely mimic a physiological condition where the cancer cells may undergo periodic or consistent nutrient replenishment.

After PEF exposure, the samples were plated in six-well plates (VWR ®), where 400 µL of the sample media was mixed with 1.6 mL of growth media, totaling 2 mL/well. Each set of parameters was tested in triplicate. We extracted 10 µL of each sample every twelve hours into an individual 0.5 mL Eppendorf tube and mixed with 10 µL of Trypan-blue to count the sample in the Countess. We report the results as the average of three samples with the standard deviation. Upon attaining 2×10^6 cells/mL, the sample was spun down, resuspended in fresh media using 2 mL Eppendorf tubes, and re-plated.

3.2.5 Mathematical Modeling of Cell Population Dynamics

As depicted in Figure 5, we consider the cancer cell population as comprised of proliferating cells that may divide or transition to quiescence and quiescent cells that may transition to proliferating or undergo irreversible death. The resulting growth kinetics may therefore be represented mathematically by a pair of coupled differential equations, given by [61], [88]

$$x'(t) = bx(t) - P(x,y)x(t) + Q(x,y)y(t) \quad (2)$$

$$y'(t) = P(x,y)x(t) - Q(x,y)y(t) - dy(t) \tag{3}$$

where $x(t)$ and $y(t)$ are the number of proliferating and quiescent cells at time t, respectively, b and d represent the rates of proliferating cell division and quiescent cell death, respectively,

$$P(x,y) = c[x(t) + ay(t)] \tag{4}$$

describes the intensity of cell transition from proliferating to quiescent, where a is the dimensionless constant that measures the nutrient uptake by all cells and c represents the rate of the transition from the proliferating to the quiescent state, and

$$Q(x,y) = \frac{Ax(t)}{1 + Bx^2(t)}. \tag{5}$$

describes the intensity of cell transition from quiescent to proliferating, $x(0)$ and $y(0)$ are the initial number of proliferating and quiescent cells, respectively, and the total number of cells given by [61], [88]

$$z(t) = x(t) + y(t). \tag{6}$$

Previous studies justified that $Q(x,y) \approx 0$ under most physically relevant conditions and that the entire cell population would eventually decay exponentially if $x(t) < c/b$ as long as $Q(x,y)$ was sufficiently small to not provide another source of proliferating cells [61]. Physically, this condition shows that once a system contains fewer than one proliferating cell and no source for creating more, the cell population will eventually decay to zero [61]. Combining (2) through (5) yields

$$x'(t) = bx(t) - c[x(t) + ay(t)]x(t) \tag{7}$$

$$y'(t) = c[x(t) + ay(t)]x(t) - dy(t). \tag{8}$$

Ref. [61] nondimensionalized (7) and (8) and showed that $r = d/b$ was an important dimensionless quantity representing the ratio of the rates of cell death d and cell division b. In this thesis, we

solved (7) and (8) to fit measured $z(t)$ over the interval of cell counts to obtain a, b, c and d using a least squares fit with a time step of 0.1 d (2.4 h).

One of the important characteristics from (7) and (8) is that $z(t)$ will ultimately reach a steady state for long time t. One can obtain these steady-state values by setting (7) and (8) to zero and solving for the resulting nontrivial steady states x_{ss} and y_{ss} of $x(t)$ and $y(t)$, respectively, given by

$$x_{ss} = \frac{db}{c(ab + d)} \tag{9}$$

$$y_{ss} = \frac{b^2}{c(ab + d)}. \tag{10}$$

The steady state value of the full population will therefore be $z_{ss} = x_{ss} + y_{ss}$. While not explicitly stated in the derivation of these equations, fitting (7) and (8) to experimental data that does not follow a standard sigmoidal shape (s-curve) is very challenging since (7) and (8) generally lead to scenarios of cell population growth.

A previous dissertation from our group [58] attempted to fit (7) and (8) to various PEF treatment scenarios with limited success. This thesis focuses on the condition where subthreshold PEFs reduce the rate of cell population growth such that the general shape remains sigmoidal (s-curve), but z_{ss} is depressed. This is an important practical consideration for clinical applications of PEFs, such as nsPEFs or irreversible electroporation, where regions of the tumor may receive subthreshold exposures and continue to undergo cell population growth following treatment. It is possible that feeding the cells daily as we are doing could increase the transition from quiescent to proliferating, which we do not explicitly consider here, but could be worth additional study.

3.3 Results

3.3.1 Determination of Initial Fractions of Proliferating and Quiescent Cells

To apply the model outlined in Section 3.2, we must first determine an appropriate initial condition for the fractions of proliferating and quiescent cells, or $x^* = x(0)/z(0)$ and $y^* = y(0)/z(0)$, respectively. A cell typically undergoes three distinct states: resting (quiescent), interphase, and cell division [89-90]. A cell is considered in the G0 (Gap 0) phase when it has left the cell cycle

and stopped dividing [89-90]. Interphase consists of the G1, S, and G2 phases. The cell grows in the G1 phase and there is a checkpoint at the end to ensure that the cell is prepared for DNA replication, which occurs in the S phase. The G2 phase is the gap between DNA synthesis and mitosis, or the M phase. For the purposes of this theory, we consider cells in the G0 phase as quiescent and the other phases, when the cells are actively growing or replicating, as proliferating. As we shall see when we summarize data on the fraction of Jurkats in the quiescent state, many studies report cells in the G0/G1 phase rather than in the G0 phase, which may date back to preliminary debate concerning the distinctness of the G0 phase [91]. Another issue is that the traditional single parameter DNA content histogram analysis using flow cytometry cannot easily distinguish G0 from G1 or G2 from M [92].

In their initial theoretical study, Solyanik et al. demonstrated that individual cell populations under the same environmental conditions could undergo different cell population dynamics due to differences in either the initial total number of cells or the proportions of quiescent and proliferating cells. They used data from Wallen et al. (1984a, 1984b) for testing their models and determined that 70% of the cells were proliferating based on DNA distribution of the cells in exponential cultures. Solyanik et al. also considered the effect of hypoxia on cell growth and estimated by data fitting that the initial fraction of proliferating cells decreased from 70% to 30% due to hypoxia.

Thus, the first challenge in performing these fits is determining an appropriate fraction of initial proliferating cells. Table 3 summarizes typical fractions of Jurkat cells in the G0 and G0/G1 phases. For the studies that distinguished the G0 from combined G0/G1 phase, the percentage of quiescent cells ranged from 5-8.4%. Except for one outlier at 16.17% [95], the percentage of Jurkat cells in the combined G0/G1 phase ranged from 40 % to 58 %. Therefore, we would anticipate $0.9 < x^* < 0.95$ for a control under typical conditions since that corresponds to the cells that we would consider quiescent by the definition above. Since Solyanik, et al. observed that they could fit hypoxic effects by a reduction in x^*, we would anticipate that PEF treatment of Jurkat cells would reduce x^* compared to the values reported here. In other words, we would anticipate $x^* \lesssim 0.9$.

Table 3: Summary of the fraction of Jurkat cells in quiescent (G0) phase or combine G0/G1 phase. N/A indicates that the study did not specifically report that fraction.

Reference	% of Cells in G0	% of Cells in G0/G1
[92]	8.4	43.2
[93]	5	55
[94]	5	N/A
[95]	N/A	16.17
[96]	N/A	48
[97]	N/A	56
[98]	N/A	46.27
[99]	N/A	54.3
[100]	N/A	58
[101]	N/A	40

We chose a fixed quiescent rate of 16.17% for all the runs from the experimental measurements reported on Jurkat cell cycle analysis [95]. Although this study reported G0/G1 and we define G0 as quiescent, this value satisfies the conditions above for $x^* \lesssim 0.9$ and is reasonable based on the observations by Solyanik, et al. Future studies will examine the impact of variations in x^* on sensitivity and fitting the other model parameters. We applied the theory in (4), (5), (7) and (8) to the experimental data for the parameters at 5 kV/cm, 20 kV/cm, and 30 kV/cm assuming that $y^* = y(0)/z(0) = 0.1617$ and $x^* = x(0)/z(0) = 0.8383$. The quality of the fit of the model to the experimental data was assessed using correlation coefficient (r^2). This is lower than predicted by Refs. [92-94], which specifically account for the quiescent state, but higher than observed by Solyanik et al., both before and after hypoxic treatment. Based on this assessment, this value seemed reasonable.

3.3.2 Fitting the Model to Experimental Data

Now that we have a reasonable value for x^*, we next fit (5) and (6) to experimental data [58] for trains of 10, 30, and 50 300 ns PEFs using a least-squares curve fit in MATLAB. We performed ten iterations of this fit with slight modifications in the initial conditions to assess the robustness of the fit, over the iterations the parameters stabilized to the final results. Moreover, we set appropriate upper and lower bounds of a, b, c, and d to prevent unphysically large or negative values. Table 4 reports the fit values of a, b, c, d, $r = d/b$, and r^2 to fit (5) and (6) to the measured cell counts assuming $x^* = 0.8383$. Note that another assumption would be fix a, b, c, and d and examine the resulting changes in x^*. The challenge with this is that PEFs may also change cellular

functions, most notably cell death rate *d* and reproduction rate *b*, so we started with this approach as being the most convenient to fit and the most likely to elucidate the implications of PEFs on these parameters.

Table 4: Values for fitting parameters obtained from fitting 300 ns, 5 kV/cm treatments experimental data to mathematical models of cell population assuming an initial cell population comprised of 84% proliferating cells with no (0) electric pulses representing the unpulsed control.

Number of Pulses	*a*	*b* (d^{-1})	*c* ($cell^{-1}\ d^{-1}$)	*d* (d^{-1})	*r*	r^2
0	0.43	0.713	0.707	4.17×10^{-7}	5.85×10^{-7}	0.9952
10	0.54	0.641	0.203	3.77×10^{-4}	5.88×10^{-4}	0.9868
30	4.88	0.701	0.280	2.05×10^{-3}	2.92×10^{-3}	0.9916
50	185	0.579	0.0192	6.21×10^{-1}	1.07	0.9918

Figures 7 and 8 show the sensitivity of the final cell concentration to these extracted parameters from Table 4 by increasing or decreasing a given parameter by 10% with all others fixed and reporting the percentage change in the total cell population at the final time point for the control and the 30 pulse data, respectively. For both conditions, changing *d* had the least effect on the calculated cell population after seven days, while *b* had the greatest effect. This suggests that the model will be more sensitive to changes in the cellular replication rate than to the death rate, while changes altering the transition between quiescent and proliferating states were generally more moderate. Most noticeable is the minimal effect of the death rate on the population outcome. Figures 9-12 show that the number of proliferating and quiescent cells both increase with time for the first 4-6 d post-treatment regardless of the number of PEFs. In Figure 9, $y(t) > x(t)$ after approximately 4.5 d for the control, indicating the transition toward the steady state since a larger population of quiescent cells is generally necessary to balance out the net growth of the full cell population. For the cases of 0, 10, and 30 PEFs, the total cell population appears to approach the final steady state population after approximately 7 d. As anticipated, the steady state population decreases with increasing number of PEFs. For 50 pulses, the results are a bit more ambiguous. While the shape of the model fit and the experimental data suggest that the total cell population is approaching a steady state, the model indicates that the cell population will decrease. The fit parameters in Table 3 may provide some insight into this behavior. The values of *b* range from 0.579 to 0.713 for all PEF trains studied here with the lowest value of 0.579 occurring after 50

pulses. This indicates that exposure to an increasing number of PEFs reduces the division rate of the proliferating cells. The most significant difference in the fitting parameters is the change in *d*, which goes from 4.17×10^{-7} d^{-1} for the control to 6.21×10^{-1} d^{-1} for 50 PEFs, changing *r* from 5.85×10^{-7} to 1.07, emphasizing the six orders of magnitude change in d between control and 50 PEFs. We note that *r* gradually increases with increasing number of PEFs, as one would expect due to the impact of the number of PEFs. Also of note is that the overall ratio of proliferating to quiescent cell is fairly constant across time for 0, 10, and 30 PEFs. This lends further credence to our selection of a fixed x^* for the initial condition for all these cases since the ratio and trends are relatively similar across time. The data for 50 PEFs requires further study as the number of quiescent cells is much higher initially than the other conditions. While this makes sense based on the biophysics involved, it is unclear how this occurred mathematically. Future studies will explore the effect of considering x^* for this condition to assess the sensitivity of the fit.

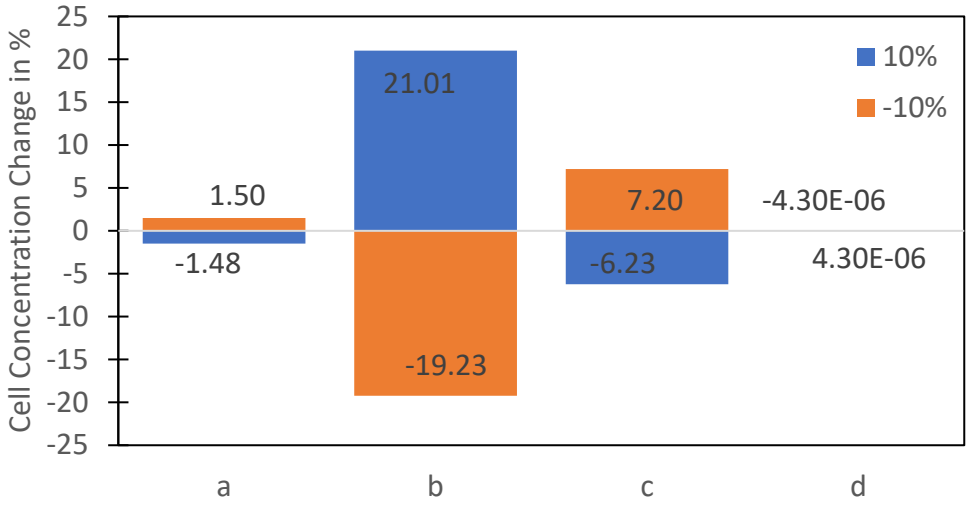

Figure 7: Percentage change in cell concentration for the control population over the experimentally measured time span by increasing or decreasing each parameter by 10% with all others fixed.

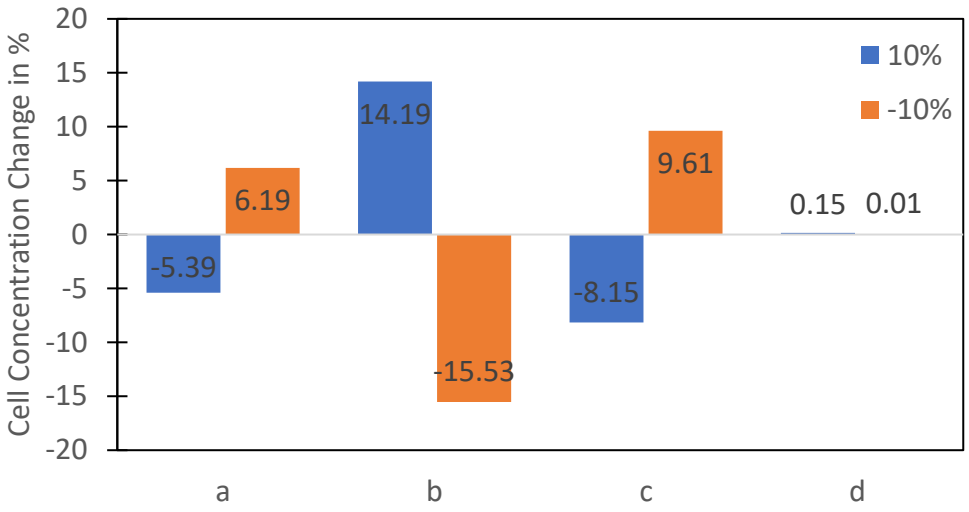

Figure 8: Percent change in cell concentration for the 300 ns 5 kV/cm 30 pulse treatment population over the experimentally measured time by increasing or decreasing each parameter 10% with all other parameters fixed.

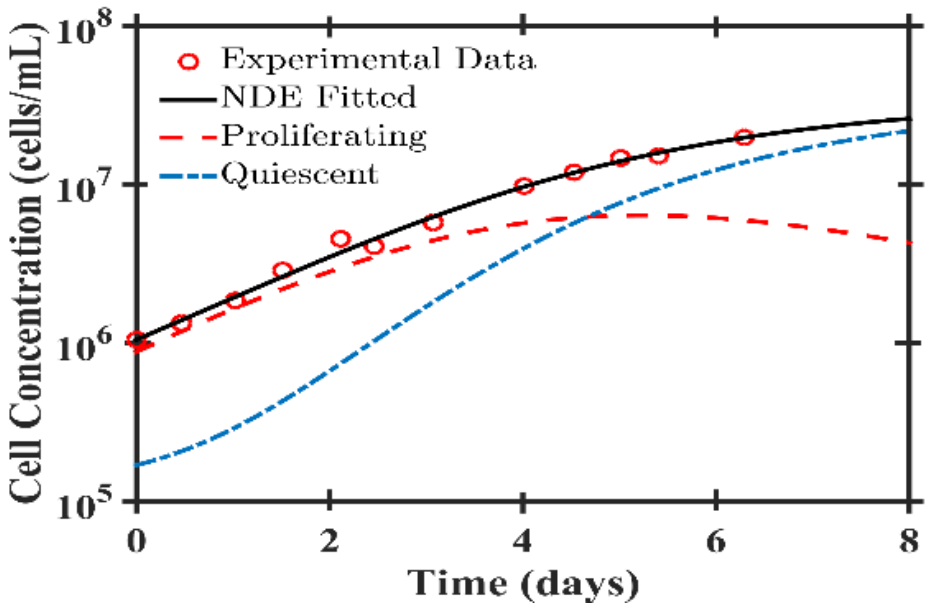

Figure 9: Growth curves and model fitting of Jurkat cells (control).

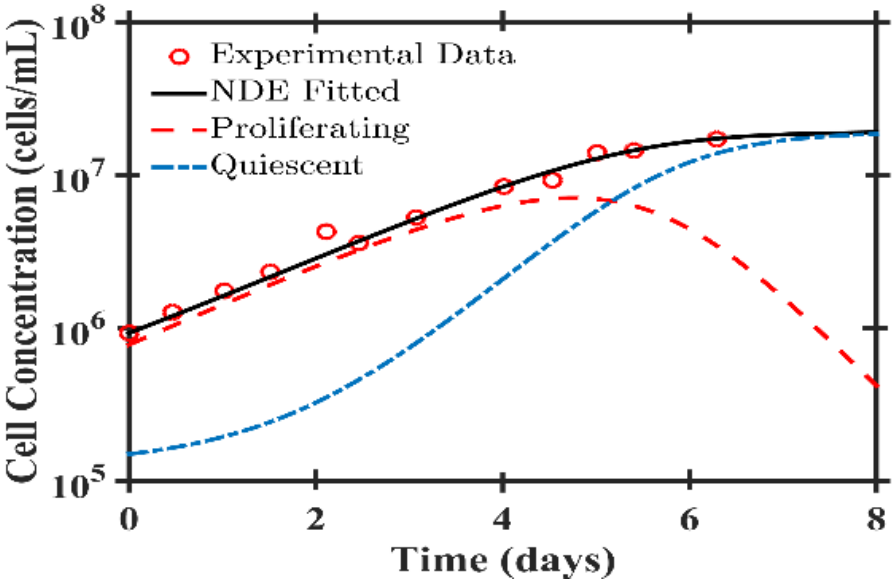

Figure 10: Growth curves and model fitting of Jurkat cells after PEF treatment: 300 ns, 5 kV/cm, 10 pulses.

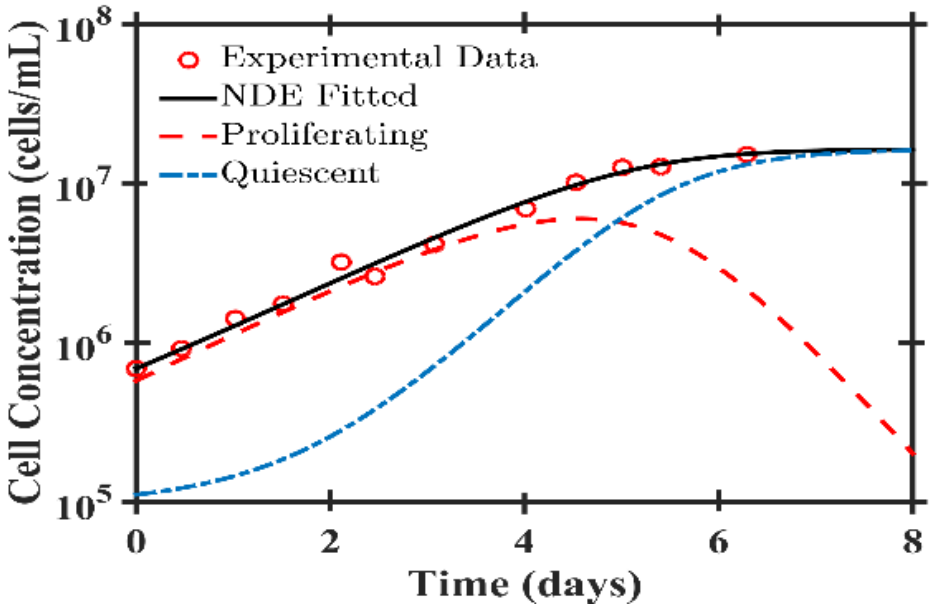

Figure 11: Growth curves and model fitting of Jurkat cells after PEF treatment: 300 ns, 5 kV/cm, 30 pulses.

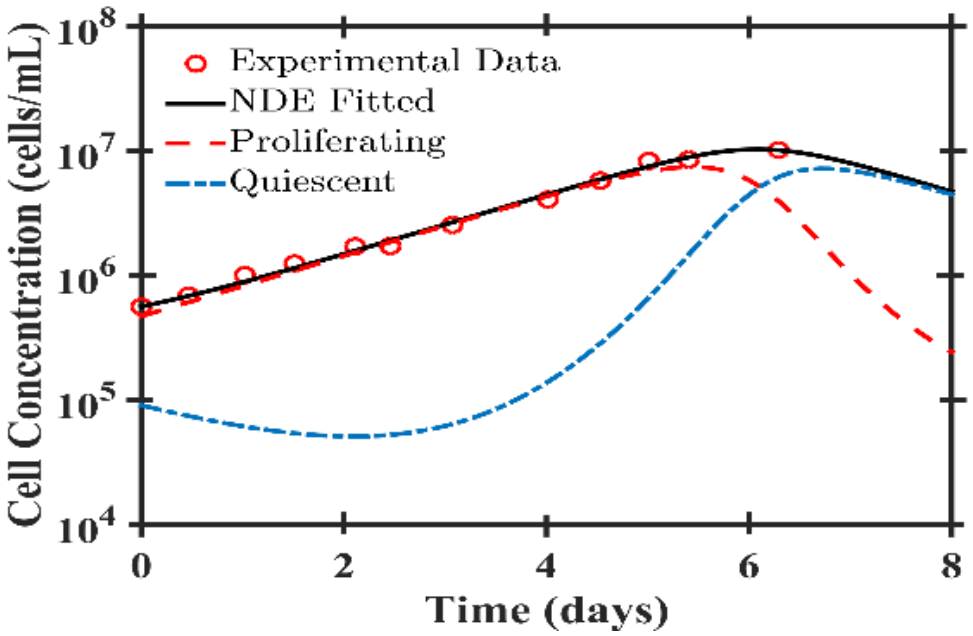

Figure 12: Growth curves and model fitting of Jurkat cells after PEF treatment: 300 ns, 5 kV/cm, 50 pulses.

One final point concerns the data itself in Figures 9-12. Although the data looks very similar, it is important to note that it is on a logarithmic scale. Thus, between these figures, the later data points may differ by several fold. This difference becomes significant when fitting the theory above to the data, resulting variations in the parameters that may seem large. Additionally, the fits show that the slopes of the line are somewhat different, with the control exhibiting a slightly sharper slope indicating that the population is still increasing compared to the PEF treatments. This highlights the advantage of applying the theory in this case to examine long-term steady state behavior due to these PEF treatments that may not necessarily be evident from the data alone. This is particularly critical for these subthreshold PEFs where the cell still approach what appears to be a reduced steady state when compared to control.

3.4 Conclusion

This Chapter showed that a simple theory for cancer cell population dynamics that considers the cells as either proliferating or quiescent may be applied to conditions for an external PEF to biological cells. This particular theory is most relevant when the cell population behaves

sigmoidally (S-curve) and not for other cases, such as when the PEFs lead to noticeable and dramatic cell population reduction [58]. Future studies may adapt this theory in a number of way.

First, the initial application of this theory by Solyanik, et al. assumed that the cells were unfed. Due to issues with cell viability, we changed the cell culture media daily. Most likely, we would anticipate that this could change each parameter within the theory since it could increase *b*, decrease *d*, and increase the transition from quiescent to proliferating. In general, we would expect many of these changes to be incorporated into the fitting and the transition from quiescent to proliferating to remain sufficiently small to be negligible. A future model could more explicitly account for this media changing, but we suspect that the changes will not be significant.

Second, as mentioned several times earlier, the model fails to adequately fit non-sigmoidal data. One way to account for this may be to more explicitly include the effect of the external stimulus. Right now, we have directly applied this theory as written to cell populations under external stimulus with no modification. A future iteration of this theory could involve adapting it account explicitly for the stimulus. The challenge with this is knowing a priori what this change will be. For instance, vast literature exists examining the interaction of PEFs with cell membranes, both examining the change in transmembrane potential and in membrane pore formation. At their root, these phenomena are directly induced by the PEFs and may be derived from known principles. In this case, the interaction with cell population dynamics is not a direct physical change; instead, it occurs due to an overall change in cellular function. This makes developing a first-principles based (or inspired) theory much more challenging. The data obtained here shows noticeably effects to *b* and *d*, but there is no clear indication of how to relate these changes to pulse parameters. Such an approach would likely need to be semi-empirical based on multiple experiments.

These two potential extensions basically emphasize the need for more detailed experiments. First, experiments using PEFs with different cell lines could be performed to examine changes in the cell cycle. This would be valuable because it could provide information on the cell cycle both in control over time and then immediately after biological cell treatment. Culturing the cells for many days and revisiting this would provide us with the ability to benchmark the model and characterize the implications of sub-threshold PEFs on therapy. At that point, the theory may be adjusted to account for PEF-induced changes in the cell cycle such that it may gain more predictive power.

Ultimately, the real significance of this work is to apply it to elucidate the implications of subthreshold conditions for PEF-induced cancer cell treatment. This has implications across PEF cancer treatment modalities, including irreversible electroporation, nsPEFs, and electrochemotherapy, because all conditions are susceptible to non-uniform field exposure. Thus, while much of a treatment area may undergo an appropriate PEF exposure for cancer treatment, areas on the periphery may not; the experiments and application of the theory presented here are a first step to characterizing these conditions. This simple theory may be used to determine the resulting steady-state population anticipated under certain sub-threshold fields to provide insight into the necessity of future treatments and the required parameters.

To transition such an approach toward clinical parameters, the next step will involve considering more realistic conditions. One such approach could be a 3D-cell culture, which possesses some of the properties of the real physiological conditions but provides much more control in the system to permit application of simple theories. Another approach could involve investigating multicellular tumor spheroids (MTS). This would involve a completely different theory, much like studied elsewhere [62] because one would then need to account for the different structures of the tumor, most notably the proliferating rim and necrotic core. MTS are equivalent to avascular tumors since they do not have blood vessels to provide nutrients, making diffusion the driving force. An artificial tumor with blood vessels would provide a more realistic model system to further examine the anti-angiogenic nature of PEFs for cancer treatment.

In conclusion, this simple theory provides some insight into the behavior of cell population over time and the implications of treatment. Additional experimental data and theoretical modification may make this model more valuable as a predictive tool. Further extension to conditions more relevant for in vivo studies, such as 3D cell culture, may ultimately provide a means to benchmark the impact of non-uniform PEF treatments to aid device and system design prior to animal and clinical studies.

4. CONCLUSION

This thesis has focused on applying nsPEFs to inactivate different cell types, specifically microorganisms in combination with antibiotics and immortalized leukemia cells (Jurkat). Specifically, it has demonstrated the broad utility of nsPEFs for these purposes and provided some important insight in future applications of antimicrobial treatments and theoretical insight into cancer cell treatment.

Chapter 2 extends prior work combining nsPEFs with antibiotics to enhance microorganism inactivation by making Gram positive antibiotics effective against Gram negative microorganisms. This has significant implications since developing new Gram-negative antibiotics is difficult. Repurposing already existing Gram-positive antibiotics by using nsPEFs to permeabilize microorganism membranes could open up new methods for addressing antibiotic resistance. Future work will involve developing PEF systems for applying this approach to surfaces and implants, including electrode systems and PEF parameter optimization, specifically pulse duration and repetition rate. Moreover, a detailed assessment of different drugs and microorganisms may lead to other applications. Additionally, different PEF parameters and synergies, such as temperatures, temperatures, and other drugs may be incorporated.

Chapter 3 outlines the application of a simple mathematical theory to subthreshold PEF treatments to Jurkat cells for characterizing the behavior of quiescent and proliferating cells following different numbers of PEFs. The theory provides insight into the long-term behavior of the cells following PEF treatment. Further experimental studies into cell state and ultimate into 3-D cell culture or multicellular tumor spheroids could provide guidance for system design and parameter selection for in vivo treatments. Of particular notes, characterization of sub-threshold PEF treatment is important for optimizing therapy. This is a particularly important consideration for treatment development.

The work can be extended by adding other treatments, such as chemotherapeutic drugs, and examining synergistic effects on cell population and the model fit parameters. Future studies may also consider the stage of the cell cycle at various points before and after PEF treatment to validate the model predictions. Of particular interest, how does changing the PEF parameters (particularly pulse duration and electric field intensity) change the stage of the cell cycle targeted? Because shorter duration PEFs target intracellular structures, would certain stages during division

when nuclear materials may be more greatly exposed be more targeted by nsPEFs than microsecond PEFs? Such studies may be undertaken by controlling the cell cycle prior to PEF treatment to examine the implications of PEFs parameters on subsequent proliferation and death. Finally, the primary motivation of this effort was to characterize the implications of subthreshold PEFs on cell population dynamics since practical PEF cancer therapies will inevitably exhibit some degree of field nonumiformity which will impact treatment efficacy. While this study provides initial insight on the resulting cell population behavior following PEF application that does not completely kill the cells, a more detailed subsequent study could examine these effects in an intermediate system between a cuvette and an in vivo, such as a multicellular tumor spheroid or a 3D cell culture. This would provide a first order test of the implications of treatment geometry and cellular alignment and interaction not present in a cuvette while avoiding the complications or expense of a physiological or clinical environment. Extending the theory of PEF parameters on cell population dynamics would provide fundamental insight that may guide clinical pulse delivery, particularly electrode design and PEF parameters.

In summary, this thesis elucidates the use of PEFs for cellular inactivation of microorganisms and cancer cells. While not the only application of PEFs, these are two critical areas in medicine and this thesis demonstrates how simple, fundamental experimental and theoretical studies can provide valuable information. Both areas could be extended for clinically relevant applications based on the results presented here.

REFERENCES

[1] A. L. Garner, G. Chen, N Chen, V Sridhara, J Kolb, R. J. Swanson, S. J. Beebe, R. P. Joshi and K.H. Schoenbach, "Ultrashort electric pulse induced changes in cellular dielectric properties," Biochem. Biophys. Res. Comm. **362,** 139-144 (2007).

[2] Y. Feldman, I. Ermolina, and Y. Hayashi, "Time domain dielectric spectroscopy study of biological systems," IEEE Trans. Dielect. Electr. Insul. **10,** 728-753 (2003).

[3] R. P. Joshi and K. H. Schoenbach, "Electroporation dynamics in biological cells subjected to ultrafast electrical pulses: A numerical simulation study," Phys. Rev. E **62**, 1025-1033 (2000).

[4] K. H. Schoenbach, R. P. Joshi, J. F. Kolb, N. Chen, M. Stacy, P. F. Blackmore, E. S. Buescher and S. J. Beebe, "Ultrashort electrical pulses open a new gateway into biological cells," Proc. IEEE **92**, 1122-1137 (2004).

[5] A. J. H. Sale and W. A. Hamilton, "Effects of high electric fields on microorganisms: I. Killing of bacteria and yeasts," Biochim. Biophs. Acta—General Subjects **148**, 781-788 (1967).

[6] W. A. Hamilton and A. J. H. Sale, "Effects of high electric fields on microorganisms: II. Mechanism of action of the lethal effect," Biochim. Biophys. Acta—General Subjects **148,** 789-800 (1967).

[7] U. Zimmermann, G. Pilwat, and F. Riemann, "Dielectric Breakdown of Cell Membranes," Biophys. J. **14**, 881-899 (1974).

[8] R. Benz, F. Beckers, and U. Zimmermann, "Reversible electrical breakdown of lipid bilayer membranes: A charge-pulse relaxation study," J. Membrane Biol. **48**, 181-204 (1979).

[9] M. R. Prausnitz, V. G. Bose, R. Langer, and J. C. Weaver, "Electroporation of mammalian skin: a mechanism to enhance transdermal drug delivery," Proc. Nat. Acad. Sci. USA **90**, 10504-10508 (1993).

[10] D. Rabussay, N. B. Dev, J. Fewell, L. C. Smith, G. Widera, and L. Zhang, "Enhancement of therapeutic drug and DNA delivery into cells by electroporation," J. Phys. D **36**, 348-363 (2003).

[11] G. Sersa, M. Cemazar, and M. Snoj, “Electrochemotherapy of tumours,” Curr. Oncol., **16**, 34-35 (2009).

[12] J. C. Weaver and Yu. A. Chizmadzhev, “Theory of electroporation: A review,” Bioelectrochem. Bioenerg. **41,** 135-160 (1996).

[13] J. Teissie, and M-P Rols, “An experimental evaluation of the critical potential difference inducing cell membrane electropermeabilization,” Biophys. J. **65**, 409-413 (1993).

[14] D. P. Tieleman, “The molecular basis of electroporation,” BMC Biochemistry **5**, 10 (2004).

[15] Z. A. Levine and P. T. Vernier, “Life cycle of an electropore: field-dependent and field-independent steps in pore creation and annihilation,” J. Membrane Bio. **236**, 27-36 (2010).

[16] P. T. Vernier, M. J. Ziegler, Y. Sun, W. V. Chang, M. A. Gundersen, and D. P. Tieleman, “Nanopore formation and phosphatidylserine externalization in a phospholipid bilayer at high transmembrane potential,” J. Am. Chem. Soc. **128**, 6288-6289 (2006).

[17] A G. Pakhomov, J. F. Kolb, J. A. White, R. P. Joshi, S. Xiao, and K. H. Schoenbach, “Long-lasting plasma membrane permeabilization in mammalian cells by nanosecond pulsed electric field (nsPEF),” Bioelectromagnetics **28**, 655-663 (2007).

[18] A. G. Pakhomov, R. Shevin, J. A. White, J. F. Kolb, O. N. Pakhomova, R. P. Joshi, and K. H. Schoenbach, K.H., 2007. Membrane permeabilization and cell damage by ultrashort electric field shocks. Arch. Biochem. Biophys. **465**, 109-118 (2007).

[19] J. Zhang, P. F. Blackmore, B. Y. Hargrave, S. Xiao, S. J. Beebe, and K. H. Schoenbach, “Nanosecond pulse electric field (nanopulse): a novel non-ligand agonist for platelet activation,” Arch. Biochem. Biophys. **471**, 240–248 (2008).

[19] A. S. Torres, A. Caiafa, A. L. Garner, S. Klopman, N. Laplante, C. Morton, K. Conway, A. D. Michelson, A. L. Frelinger, and V. B. Neculaes, “Platelet activation using electric pulse stimulation: Growth factor profile and clinical implications,” J. Trauma Acute Care Surg. **77**, S94–S100 (2014).

[20] A. L. Frelinger III, A. J. Gerrits, A. L. Garner, A. S. Torres, A. Caiafa, C. A. Morton, M. A. Berny-Lang, S. L. Carmichael, V. B. Neculaes, and A. D. Michelson, “Modification of pulsed electric field conditions results in distinct activation profiles of platelet-rich plasma,” PLoS ONE **11**, e0160933 (2016).

[21] A. L. Garner, A. L. Frelinger III, A. J. Gerrits, T. Gremmel, E. E. Forde, S. L. Carmichael, A. D. Michelson, and V. B. Neculaes, "Using extracellular calcium concentration and electric pulse conditions to tune platelet-rich plasma growth factor release and clotting," Med. Hypotheses **125**, 100-105 (2019).

[22] M. J. Blaser, *Missing Microbes: How Killing Bacteria Creates Modern Plagues* (Oneworld, London, 2014).

[23] A. Fleming, Nobel lecture on penicillin, (PA Norstedt & Söner, 1947).

[24] T. Kostyanev, and F. Can, "The global crisis of antimicrobial resistance," Antimicrob Steward 2, 3-12 (2017).

[25] R. Aminov, "History of antimicrobial drug discovery: Major classes and health impact," Biochem.. Pharmacol **133**, 4–19 (2017).

[26] W. Witte, "Medical consequences of antibiotic use in agriculture," Science **279,** 996–997 (1998).

[27] CDC, "Antibiotic Resistance Threats in the United States," (2013).

[28] D. S. Davies, and E. S. Verde, "Antimicrobial resistance. Search Collab Solut World Innov Summit Health Doha, 1–36 (2013).

[29] M. Z. David, M. Dryden, T. Gottlieb, P. Tattevin, and I. M. Gould, "Recently approved antibacterials for methicillin-resistant *Staphylococcus aureus* (MRSA) and other Gram-positive pathogens: the shock of the new," Int. J. Antimicrob. Agents **50**, 303–307 (2017).

[30] WHO, "The selection and use of essential medicines: report of the WHO Expert Committee," (2017).

[31] H. Mohammad, A. AbdelKhalek, N. S. Abutaleb, and M. N. Seleem, "Repurposing niclosamide for intestinal decolonization of vancomycin-resistant enterococci," Int. J. Antimicrob. Agents **51**, 897–904 (2018).

[32] S. Thangamani, H. Mohammad, M. F. Abushahba, T. J. Sobreira, and M. N. Seleem, "Repurposing auranofin for the treatment of cutaneous *staphylococcal* infections," Int. J. Antimicrob. Agents **47**, 195–201 (2016).

[33] A. Vadlamani, D. A. Detwiler, A. Dhanabal, and A. L. Garner, "Synergistic bacterial inactivation by combining antibiotics with nanosecond electric pulses," Appl. Microbiol. Biotechnol. **102**, 7589–7596 (2018).

[34] A. L. Garner, "Pulsed electric field inactivation of microorganisms: from fundamental biophysics to synergistic treatments," Appl. Microbiol. Biotechnol. **103**, 2917-2929 (2019)

[35] M. Birbir, H. Hacıoğlu, Y. Birbir, and G. Altuğ, "Inactivation of *Escherichia coli* by alternative electric current in rivers discharged into sea," J. Electrost. **67**, 640–645 (2009).

[36] M. Amiali, M. O. Ngadi, J. P. Smith, and G.S. V. Raghavan. "Synergistic effect of temperature and pulsed electric field on inactivation of Escherichia coli O157: H7 and Salmonella enteritidis in liquid egg yolk," J. Food Eng. **79**, 689–694 (2007).

[37] M. Walkling-Ribeiro, O. Rodríguez-González, S. H. Jayaram, and M. W. Griffiths, "Processing temperature, alcohol and carbonation levels and their impact on pulsed electric fields (PEF) mitigation of selected characteristic microorganisms in beer," Food Res. Int. **44**, 2524–2533 (2011).

[38] Q. Zhang, B. L. Qin, G. V. Barbosa-Canovas, and B. G. Swanson, "Inactivation of E. coli for food pasteurization by high-strength pulsed electric fields," J Food Process. Preserv. **19**, 103–118 (1995).

[39] I. Francolini and G. Donelli, "Prevention and control of biofilm-based medical-device-related infections," FEMS Immunol. Med. Microbiol. **59**, 227–238 (2010).

[40] J. L. del Pozo , M. S. Rouse, J. N. Mandrekar, M. F. Sampedro, J. M. Steckelberg, and R. Patel, "Effect of electrical current on the activities of antimicrobial agents against Pseudomonas aeruginosa, Staphylococcus aureus, and Staphylococcus epidermidis biofilms," Antimicrob. Agents Chemother. **53**, 35–40 (2009).

[41] J. F. Kolb, S. Kono, K. H. Schoenbach, "Nanosecond pulsed electric field generators for the study of subcellular effects," Bioelectromagnetics **27**, 172–187 (2006).

[42] S. Hughes, K. Heard, and L. S. Moore, "Antimicrobial therapies for Gram-positive infections," Lung Cancer **15**, (2018).

[43] S. Perni, P. R. Chalise, G. Shama, and M. G. Kong, "Bacterial cells exposed to nanosecond pulsed electric fields show lethal and sublethal effects," Int. J. Food Microbiol. **120**, 311–314 (2007).

[44] K. H. Schoenbach, R. P. Joshi, S. J. Beebe, and C. E. Baum, "A scaling law for membrane permeabilization with nanopulses," IEEE Trans Dielectr Electr Insul **16**, 1224–1235 (2009).

[45] J. C. Weaver and Y. A. Chizmadzhev, "Theory of electroporation: a review," Bioelectrochem. Bioenerg. **41**, 135–160 (1996).

[46] B. Goldstein, “Resistance to rifampicin: a review,” J. Antibiot. **67**, 625–630 (2014).

[47] P. Alifano, C. Palumbo, D. Pasanisi, and A. Talà, “Rifampicin-resistance, rpoB polymorphism and RNA polymerase genetic engineering,” J Biotechnol **202**, 60-77 (2015).

[48] K. H. Schoenbach, F. E. Peterkin, R. W. Alden III, and S. J. Beebe, “The effect of pulsed electric fields on biological cells: experiments and applications,” IEEE Trans. Plasma Sci. **25**, 284–292 (1997).

[49] J. L. del Pozo, M. S. Rouse, and R. Patel, Bioelectric effect and bacterial biofilms. A systematic review,” Int. J. Artif. Organs **31**, 786 (2008).

[50] V. Novickij, J. Švedienė, A. Paškevičius , S. Markovskaj, E. Lastauskienė, A. Zinkevičienė, I. Girkontaitė, and J. Novickij, “Induction of different sensitization patterns of MRSA to antibiotics using electroporation,” Molecules **23**, 1799 (2018a).

[51] V. Novickij, A. Zinkevičienė, R. Stanevičienė, R. Gruškienė, E. Servienė, I. Vepštaitė-Monstavičė, T. Krivorotova, E. Lastauskienė, J. Sereikaitė, and I. Girkontaitė, “Inactivation of Escherichia coli using nanosecond electric fields and nisin nanoparticles: a kinetics study” Front. Microbiol. **9**, 3006 (2018b).

[52] J. Song, R. P. Joshi, and K. H. Schoenbach, “Synergistic effects of local temperature enhancements on cellular responses in the context of high-intensity, ultrashort electric pulses,” Med. Biol. Eng. Comput. **49**, 713–718 (2011).

[53] A. L. Garner, M. Deminsky, V. B. Neculaes, V. Chashihin, A. Knizhnik, and B. Potapkin, “Cell membrane thermal gradients induced by electromagnetic fields,” J. Appl. Phys. **113**, 214701 (2013).

[54] J. Song, A. L. Garner, and R. P. Joshi, “Effect of thermal gradients created by electromagnetic fields on cell-membrane electroporation probed by molecular-dynamics simulations,” Phys. Rev. Appl. **7**, 024003 (2017).

[55] A. L. Garner, A. Caiafa, Y. Jiang, S. Klopman, C. Morton, A. S. Torres, A. M. Loveless, and V. B. Neculaes, “Design, characterization and experimental validation of a compact, flexible pulsed power architecture for ex vivo platelet activation,” PLoS ONE **12**, e0181214 (2017).

[56] M. Coustets, V. Ganeva, B. Galutzov, J. Teissie, “Millisecond duration pulses for flow-through electro-induced protein extraction from E. coli and associated eradication,” Bioelectrochemistry **103**, 82–91 (2015).

[57] E. Kvam, B. Davis, F. Mondello, and A. L. Garner, "Nonthermal atmospheric plasma rapidly disinfects multidrug-resistant microbes by inducing cell surface damage," Antimicrob. Agents Chemother. **56**, 2028–2036 (2012).

[58] R. A. Vadlamani, Assessing novel bioelectric effects of nanosecond pulsed electric fields on cell stimulation, proliferation and microorganism inactivation, dissertation, 2018.

[59] J. P. Freyer and R. M. Sutherland, "Regulation of growth saturation and development of necrosis in EMT6/Ro multicellular spheroids by the glucose and oxygen supply," Cancer Res. **46**, 3504–3512 (1986).

[60] A. M. Luciani, A. Rosi, P. Matarrese, G. Arancia, L. Guidoni, and V. Viti, "Changes in cell volume and internal sodium concentration in HeLa cells during exponential growth and following lonidamine treatment," Eur. J. Cell Biol. **80**, 187–195 (2001).

[61] A. L. Garner, Y. Y. Lau, D. W. Jordan, M. D. Uhler, and R. M. Gilgenbach, "Implications of a simple mathematical model to cancer cell population dynamics," Cell Prolif. **39**, 15–28 (2006).

[62] A. L. Garner, Y. Y. Lau, T. L. Jackson, M. D. Uhler, D. W. Jordan, and R. M. Gilgenbach, "Incorporating spatial dependence into a multicellular tumor spheroid growth model," J. Appl. Phys. **98**, 124701 (2005).

[63] M. V. Blagosklonny, "Target for cancer therapy: proliferating cells or stem cells," Leukemia **20**, 385–391 (2006).

[64] R. J. Jones, W. H. Matsui, and B. D. Smith, "Cancer stem cells: are we missing the target?" J. Natl. Cancer Inst. **96**, 583–585 (2004).

[65] J. Massagué, "G1 cell-cycle control and cancer," Nature **432**, 298–306 (2004).

[66] C. Sawyers, "Targeted cancer therapy," Nature **432**, 294–297 (2004).

[67] E. Batlle and H. Clevers, "Cancer stem cells revisited," Nat. Med. **23**, 1124 (2017).

[68] G. J. Yoshida and H. Saya, "Therapeutic strategies targeting cancer stem cells," Cancer Sci. **107**, 5–11 (2016).

[69] M. S. Sosa, P. Bragado, and J. A. Aguirre-Ghiso, "Mechanisms of disseminated cancer cell dormancy: an awakening field," Nat. Rev. Cancer **14**, 611–622 (2014).

[70] J. A. Aguirre-Ghiso, "Models, mechanisms and clinical evidence for cancer dormancy," Nat. Rev. Cancer **7**, 834–846 (2007).

[71] J. A. Hensel, T. W. Flaig, and D. Theodorescu, “Clinical opportunities and challenges in targeting tumour dormancy,” Nat. Rev. Clin. Oncol. **10**, 41–51 (2013).

[72] A. C. Yeh and S. Ramaswamy, “Mechanisms of cancer cell dormancy—another hallmark of cancer?” Cancer Res. **75**, 5014–5022 (2015).

[73] C. A. Schiffer, “BCR-ABL tyrosine kinase inhibitors for chronic myelogenous leukemia,” N. Engl. J. Med. **357**, 258–265 (2007).

[74] F. Michor, T. P. Hughes, Y Iwasa, S Branford, N. P. Shah, and C. L. Sawyers, “Dynamics of chronic myeloid leukaemia,” Nature **435**, 1267–1270 (2005).

[75] C. C. Roth, G. P. Tolstykh, J. A. Payne, M. A. Kuipers, G. L. Thompson, M. N. Desilva, and B. L. Ibey, “Nanosecond pulsed electric field thresholds for nanopore formation in neural cells,” J. Biomed. Opt. **18**, 035005–035005 (2013).

[76] T. B. Napotnik, Y. H. Wu, M. A. Gundersen, D. Miklavčič, and P. T. Vernier, “Nanosecond electric pulses cause mitochondrial membrane permeabilization in Jurkat cells,” Bioelectromagnetics **33,** 257–264 (2012).

[77] R. Nuccitelli, M. Kreis, B. Athos, R. Wood, J. Huynh, K. Lui, P. Nuccitelli and E. Epstein, “Nanoelectroablation for human carcinoma therapy,” in SPIE BiOS **8585**, 85850G–85850G (2013).

[78] S. Wu, Y. Wang, J. Guo, Q. Chen, J. Zhang, and J. Fang, “Nanosecond pulsed electric fields as a novel drug free therapy for breast cancer: an in vivo study,” Cancer Lett. **343**, 268–274 (2014).

[79] M. Stacey, J. Stickley, P. Fox, V. Statler, K. Schoenbach, S. Beebe, and S. Buescher, “Differential effects in cells exposed to ultra-short, high intensity electric fields: cell survival, DNA damage, and cell cycle analysis,” Mutat. Res. Toxicol. Environ. Mutagen. **542**, 65–75 (2003).

[80] M. R. Love, S. Palee, S. C. Chattipakorn, and N. Chattipakorn, “Effects of Electrical Stimulation on Cell Proliferation and Apoptosis,” J. Cell. Physiol. **233**, 1860 (2017).

[81] M. Cemazar and G. Sersa, “Recent advances in electrochemotherapy,” Bioelectricity **1**, 204-213 (2019).

[82] B. Markelc, M. Čemažar, G. Serša, *Effects of Reversible and Irreversible Electroporation on Endothelial Cells and Tissue Blood Flow*. (Springer, Cham, 2017).

[83] Z. Ren, X. Chen, G. Cui, S. Yin, L. Chen, J. Jiang, Z. Hu, H. Xie, S. Zheng, and L. Zhou. "Nanosecond pulsed electric field inhibits cancer growth followed by alteration in expressions of NF-κB and Wnt/β-catenin signaling molecules," PLoS ONE **8**, e74322 (2013).

[84] W. Ren, N. M. Sain, and S. J. Beebe, "Nanosecond pulsed electric fields (nsPEFs) activate intrinsic caspase-dependent and caspase-independent cell death in Jurkat cells. Biochem. Biophys. Res. Commun. **421**, 808-812 (2012).

[85] S. J. Beebe, N. M. Sain, and W. Ren, "Induction of cell death mechanisms and apoptosis by nanosecond pulsed electric fields (nsPEFs)," Cells **2**, 136-162 (2013).

[86] O. N. Pakhomova, B. W. Gregory, V. A. Khorokhorina, A. M. Bowman, S. Xiao, and A. G. Pakhomov, "Electroporation-induced electrosensitization," PLoS ONE **6**, e17100 (2011).

[87] J. Song, A. L. Garner, and R. P. Joshi, "Effect of thermal gradients created by electromagnetic fields on cell-membrane electroporation probed by molecular-dynamics simulations," Phys. Rev. Appl. **7**, 024003 (2017).

[88] G. I. Solyanik, N. M. Berezetskaya, R. I. Bulkiewicz, and G. I. Kulik, "Different growth patterns of a cancer cell population as a function of its starting growth characteristics: analysis by mathematical modelling," Cell Prolif. **28**, 263-278 (1995).

[89] J. P. Matson and J. G. Cook, "Cell cycle proliferation decisions: The impact of single cell analyses," FEBS J **284**, 362-375 (2017).

[90] H. Lodish, A Berk, S. L. Zipursky, P. Matsudaira, D. Baltimore, and J. E. Darnell, Molecular Cell Biology, 4th edition, W. H. Freeman and Company, 1999.

[91] H. M. Patt and H. Quastler, "Radiation effects on cell renewal and related systems," Physiol. Rev. **43**, 357-396 (1963).

[92] L. Qiu, M. Liu, and K. Pan, "A triple staining method for accurate cell cycle analysis using multiparamter flow cytometry," Molecules **18**, 15412-15421 (2013).

[93] X. Zhang, Y. Liu, Y. Si, X. Chen, Z. Li, L. Gao, L. Ga, and C. Zhang, "Effect of Cx43 gene-modified leukemic bone marrow stromal cells on the regulation of Jurkat cell line in vitro," Leuk. Res **36**, 198-204 (2012).

[94] M. R. Ricciardi, R. Licchetta, S. Mirabilii, M. Scarpari, A. Parroni, A. A. Fabbri, P. Cescutti, M. Reverberi, C. Fanelli, and A. Tafuri, “Preclinical antileukemia activity of tramesan: a newly identified bioactive fungal metabolite,” Oxid. Med. Cell Longev. **2017**, 1 (2017).

[95] M. Geethangili, Y. K. Rao, S. Fang, and Y. Tzeng, “Cytotix Constituents from Andrographis paniculate induce cell cycle arrest in Jurkat cells,” Phytother. Res. **22**, 1336 – 1341 (2008).

[96] C. B. Pereira, C. C. Kanunfre, P. V. Farago, D. M. Borsato, J. M. Budel, B. H. L. de Noronha Sales, E. A. Campesattov, A. Sartoratto, M. D. Miguel, and O. G. Miguel, “Cytotoxic mechanism of Baccharis milleflora (Less.) DC. essential oil,” Toxicology in Vitro **42**, 214-221 (2017).

[97] Z. Fang, F. Xing, C. Bronner, Z. Teng, and Z. Guo, “ICBP90 mediates the ERK1/2 signaling to regulate the proliferation of Jurkat T cells,” Cellular Immunology **257**, 80- 87 (2009).

[98] A. Costa, L. D. Chiaradia-Delatorre, L. dos Santos Bubniak, A. Mascarello, M. A. L. Marzarotto, A. C. R. de Moraes, T. R. Stumpf, M. N. S. Cordeiro, R. A. Yunes, R. J. Nunes, and M. C. Santos-Silva, “Apoptotic effect of synthetic 2′, 4′, 5′-trimethoxychalcones in human K562 and Jurkat leukemia cells,” Med. Chem. Res. **23**, 4301-4319 (2014).

[99] F. Neumann and U. Krawinkel, “Constitutive expression of human ribosomal protein l7 arrests the cell cycle in G1 and induces apoptosis in Jurkat T-lymphoma cells,” Exp. Cell Res. **230**, 252-261 (1997).

[100] F. Spinozzi, M. C. Pagliacci, G. Migliorati, R. Moraca, F. Grignani, C. Riccardi and I. Nicoletti, “The natural tyrosine kinase inhibitor genistein produces cell cycle arrest and apoptosis in Jurkat T-leukemia cells,” Leukemia Res. **18**, 431-439 (1994).

[101] B. Comín-Anduix, L.G. Boros, S. Marin, J. Boren, C. Callol-Massot, J. J. Centelles, J. L. Torres, N. Agell, S. Bassilian, and M. Cascante, “Fermented wheat germ extract inhibits glycolysis/pentose cycle enzymes and induces apoptosis through poly (ADP-ribose) polymerase activation in Jurkat T-cell leukemia tumor cells,” J. Biol. Chem. **277**, 46408-46414 (2002).

[102] C. H. Geissler, M. L. Mulligan, Z. E. Zmola, S. Ray, J. A. Morgan, and A. L. Garner, “Nanosecond and microsecond electric pulse pretreatment for enhanced lipid recovery from C*hlorella protothecoides*,” BioEnerg. Res., Accepted 19 October 2019. https://doi.org/10.1007/s12155-019-10064-z

VITA

Education:
Purdue University West Lafayette, IN 47907
Master of Science – Agricultural and Biological Engineering, Anticipated May. 2020
BS Biomedical Engineering, December 2016

Research Experience:
BioElectrics and ElectroPhysics Laboratory (BEEP) Aug. 2016 to Present
Graduate Research Assistant under Dr. Allen Garner

- Maintained cancer cell, primary stem cell, and microbial cell lines
- Assisted in pulsed power experiments and diagnostics of high voltage equipment
- Developed experimental testing protocols to assess in vitro effects of nanosecond pulsed electric fields
- Trained students in cell culture and sterile techniques
- Worked on collaborative projects between university and industry

Publications:

R. A. Vadlamani, A. Dhanabal, D. Detwiler, R. Pal, J. McCarthy, M. N. Seleem, and A. L. Garner, "Nanosecond electric pulses rapidly enhance the inactivation of Gram-negative bacteria using Gram-positive antibiotics," Applied Microbiology and Biotechnology 104, 2217–2227 (2020).

R. A. Vadlamani, Y. Nie, D. A. Detwiler, A. Dhanabal, A. M. Kraft, S. Kuang, T. P. Gavin, and A. L. Garner, "Nanosecond Electric Pulse Induced Proliferation and Differentiation of Osteoblasts and Myoblasts," Journal of the Royal Society Interface 16, 20190079 (2019).

R. S. Brayfield, II, A. J. Fairbanks, A. M. Loveless, S. Gao, A. Dhanabal, W. Li, C. Darr, W. Wu, and A. L. Garner, "The Impact of Cathode Surface Roughness and Multiple Breakdown Events on Microscale Gas Breakdown at Atmospheric Pressure," Journal of Applied Physics 125, 203302 (2019).

A. Vadlamani, D. A. Detwiler, A. Dhanabal, and A. L. Garner, "Synergistic Bacterial Inactivation by Combining Antibiotics with Nanosecond Electric Pulses," Applied Microbiology and Biotechnology 102, 7589-7596 (2018).